Journal Pre-proof

The long life of SAMBA connection in Columbia: A Paleomagnetic Study of the 1535 Ma Mucajaí Complex, Northern Amazonian Craton, Brazil

Franklin Bispo-Santos, Manoel S. D'Agrella-Filho, Lauri J. Pesonen, Johanna M. Salminen, Nelson J. Reis, Julia Massucato Silva

PII: S1342-937X(19)30281-3

DOI: https://doi.org/10.1016/j.gr.2019.09.016

Reference: GR 2229

To appear in: *Gondwana Research*

Received Date: 29 March 2019

Revised Date: 28 August 2019

Accepted Date: 21 September 2019

Please cite this article as: Bispo-Santos, F., D'Agrella-Filho, M.S., Pesonen, L.J., Salminen, J.M., Reis, N.J., Silva, J.M., The long life of SAMBA connection in Columbia: A Paleomagnetic Study of the 1535 Ma Mucajaí Complex, Northern Amazonian Craton, Brazil, *Gondwana Research*, https://doi.org/10.1016/j.gr.2019.09.016.

This is a PDF file of an article that has undergone enhancements after acceptance, such as the addition of a cover page and metadata, and formatting for readability, but it is not yet the definitive version of record. This version will undergo additional copyediting, typesetting and review before it is published in its final form, but we are providing this version to give early visibility of the article. Please note that, during the production process, errors may be discovered which could affect the content, and all legal disclaimers that apply to the journal pertain.

© 2019 Published by Elsevier B.V. on behalf of International Association for Gondwana Research.

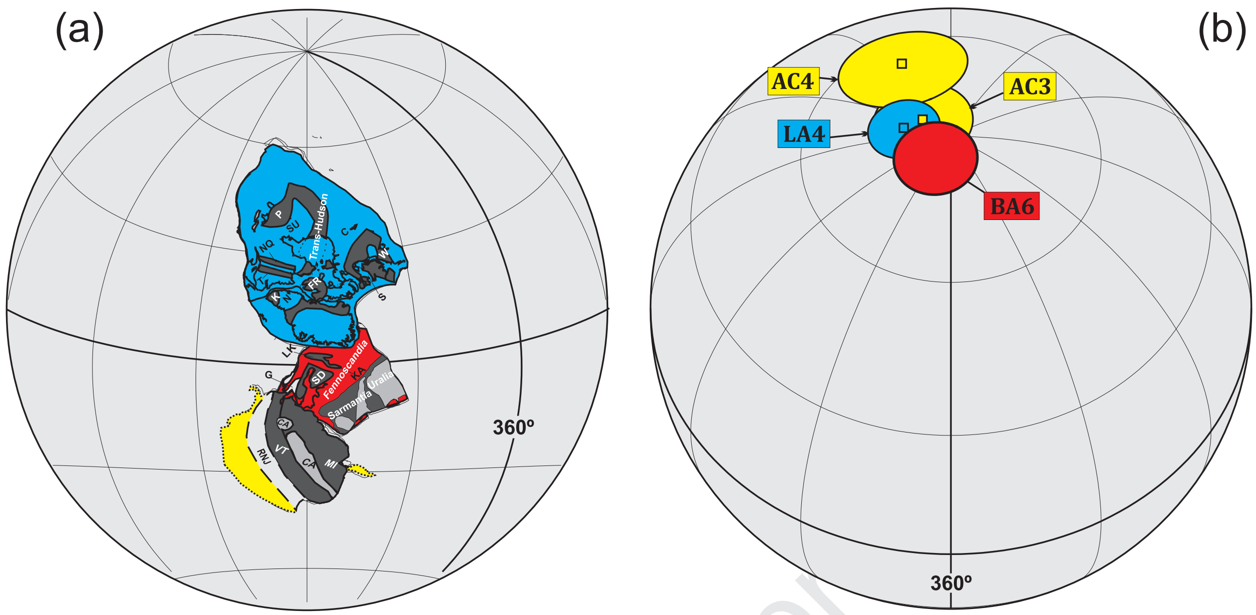

Journal Pre-proof

Journal Pre-proof

The long life of SAMBA connection in Columbia: A Paleomagnetic Study of the 1535 Ma Mucajaí Complex, Northern Amazonian Craton, Brazil

Franklin Bispo-Santos[1], Manoel S. D'Agrella-Filho[1], Lauri J. Pesonen[2], Johanna M. Salminen[2,3], Nelson J. Reis[4], Julia Massucato Silva[1]

[1]Instituto de Astronomia, Geofísica e Ciências Atmosféricas, Universidade de São Paulo, Rua do Matão, 1226, São Paulo, SP, 05508-090, Brazil.

[2]Physics Department, University of Helsinki, P.O. Box 64, 00014, Finland.

[3]Departament of Geosciences and Geography, University of Helsinki, P.O. Box 64, 00014, Finland

[4]Geological Survey of Brazil, Manaus Agency, Av. André Araújo, 2160, Manaus, Amazonas, Brazil.

Correspondent author: frankb@iag.usp.br[1]

ABSTRACT

In recent years, there has been a significant increase in the paleomagnetic data of the Amazonian Craton, with important geodynamic and paleogeographic implications for the Paleo-Mesoproterozoic Columbia supercontinent (a.k.a., Nuna, Hudsoland). Despite recent increase of paleomagnetic data for several other cratons in Columbia, its longevity and the geodynamic processes that resulted in its formation are not well known. A paleomagnetic study was performed on rocks from the ~1535 Ma AMG (Anorthosite-Mangerite-Rapakivi Granite) Mucajaí Complex located in the Roraima State (Brazil), in the northern portion of the Amazonian Craton, the Guiana Shield. Thermal and AF treatments revealed northwestern/southeastern directions with upward/downward inclinations for samples from twelve sites. This characteristic remanent magnetization is mainly carried by Ti-poor magnetite and in a lesser amount by hematite. Site mean directions were combined with previous results obtained for three other sites from the Mucajaí Complex, producing the dual polarity mean direction: Dm=132.2°; Im=35.4° (N=15; α_{95}=12.7°; k = 10.0) and a paleomagnetic pole located at 0.1°E, 38.2°S (A_{95}=12.6°; K=10.2). The Mucajaí pole favours the SAMBA (South AMerica-BAltica) link in a configuration formed by Amazonia and Baltica in Columbia. Also, there is geological and paleomagnetic evidence that the juxtaposition

Journal Pre-proof

of Baltica and Laurentia at 1.76 – 1.26 Ga forms the core of Columbia. The present paleomagnetic data predict a long life 1.78 – 1.43 Ga SAMBA connection forming part of the core of the supercontinent.

Keywords: *Paleomagnetism, Mucajaí AMG Complex, Amazonian Craton, Columbia Supercontinent*.

1. Introduction

The Amazonian Craton, the largest cratonic unit in South America, is an important unit of the supercontinental reconstructions. Its geological evolution bears little resemblance to that observed in the other South American cratonic units, but more to other cratonic blocks such as Laurentia, Baltica and West-Africa. The coeval geologic events (*e.g.,* Paleo- to Mesoproterozoic mobile belts) recorded in these presently separated continental blocks are linked together forming parts of the Proterozoic supercontinents (*e.g.,* Columbia, Nuna, Rodinia) in several proposed paleogeographic reconstructions (*e.g*., Hoffman, 1991; Buchan et al., 2000; Rogers and Santosh, 2002, 2009; Meert, 2002, 2012; Zhao et al, 2002; Pesonen et al., 2012; Johansson, 2009, 2014; Evans, 2013; Zhang et al., 2012, Xu et al., 2014, Bispo-Santos et al., 2014a; Pehrsson et al., 2016; Meert and Santosh, 2017; and references therein). This is the case for the Paleoproterozoic SAMBA model, where the Amazonian and West-African Cratons are linked to Baltica based on geological evidence (Johansson, 2009). In addition, Baltica and Laurentia are thought to form the core of Columbia in the geologically supported, long lasting (ca. 1800-1270) Ma North Europe – North America (NENA) connection (Gower et al., 1990; Salminen and Pesonen, 2007; Evans and Pisarevsky, 2008; Salminen et al., 2009, and Pisarevsky and Bylund, 2010). Paleomagnetic data for the 1790 Ma Avanavero event from northern Amazonian craton corroborate a SAMBA-like model (Reis et al., 2013; Bispo-Santos et al., 2014a). Also, the 1440-1420 Ma Amazonian paleomagnetic data agree with the SAMBA model, although some internal rotations of Amazonia relative to Baltica is suggested (D'Agrella-Filho et al., 2016a, b).

An important evidence of correlation between cratonic blocks is associated to the 1600-1400 Ma AMCG (Anorthosite-Mangerite-Charnockite-Rapakivi Granite) Complexes, which are found in several cratonic areas in the world – e.g., Baltica, Australia, North China and North America (Emslie et al., 1994; Shumlyanskyy et al., 2017). In the Amazonian Craton, AMCG's complexes are described in Rondônia (Rizzotto et al., 1996; Bettencourt et al., 1999; Scandolara et al., 2013) and in Roraima (Fraga, 2002; Fraga et al., 2009a, b; Heinonen et al., 2012), respectively, in the Central Brazil and Guiana Shields.

In the Roraima State, the Middle Proterozoic AMG activity is represented by the 1530-1540 Ma Mucajaí Complex. Coeval rocks are also described in Venezuela (Parguaza Rapakivi Granite) (Gaudette et al., 1978) and at the boundary between Venezuela and Brazil, known as Surucucus Suite (Dall'Agnol et al., 1975). All these rocks are considered to represent a single intraplate magmatic event (Gaudette et al., 1978; Dall'Agnol et al., 1999; Heinonen et al., 2012).

Here, we present a paleomagnetic study of rocks from the ~1535 Ma AMG Mucajaí Complex, located in the northern Amazonian Craton (Roraima State, Brazil). The Mucajaí Complex has already been the subject of a pilot paleomagnetic study carried out by Veikkolainen et al. (2011), whose results seem to reinforce the SAMBA-like model. However, these authors presented coherent results for only three sites of the Mucajaí Complex which did not eliminate the paleosecular variation of the geomagnetic field. The preliminary results justify a more detailed sampling of this unit, aiming to determine a key paleomagnetic pole for the Amazonian Craton, and to test the SAMBA model at 1535 Ma ago and its longevity in the Columbia supercontinent.

2. Geologic Settings

The Amazonian Craton is one of the largest cratonic areas in the world, with more than $4x10^6$ km^2. It is exposed in two large areas, the Guiana Shield to the north and the Guaporé or Central-Brazil Shield to the south, interposed by the Amazon Basin (Almeida et al., 1981). At present, there are two models that subdivide the Amazonian Craton into geotectonic and geochronological provinces, mainly based on geochronological data: one proposed by Tassinari and Macambira (1999, 2004) and another by Santos et al. (2000; 2006 and references therein). Fig. 1a shows the Amazonian Craton subdivided into tectonic provinces according to Tassinari and Macambira (1999, 2004) which was afterwards used by other authors (e.g., Schobbenhaus et al., 2004; Cordani and Teixeira, 2007; Cordani et al., 2010; Bettencourt et al., 2010). More recently, however, Fraga et al. (2008, 2009c) proposed a new evolution model for the Guiana Shield. According to Fraga et al. (2008; 2009c), the Cauarane-Coeroeni Belt (CCB) is the main tectonic feature of the central portion of the Shield, surrounded to the north and south by igneous belts where older inliers (as Trairão – T and Anauá - A) are present (Fig. 1b). The CCB is represented by high-grade supracrustal rocks disposed in a sinuous structure along the Brazil, Guyana and Suriname. The NW-SE/E-W/NE-SW trend largely fits to the major lineaments as from aeromagnetic data.

Fraga et al. (2009c, 2017) interpreted the belt as the result of the closure of an orogenic basin around 2.0 Ga during the development of the Orosirian magmatic arcs at 2.04-2.03 Ga with Rhyacian blocks to the east of the Guiana Shield. They admit a post-collisional transpressional setting for the Igneous Belts.

These Early Orosirian magmatic arcs are represented by granitoid complexes (named Trairão and Anauá) with geochemical/isotopic signature of subduction-related rocks that occur in the vicinity of the CCB or to the south of this belt. A major post-collisional magmatism, consisting of volcanic rocks and granitoids with calc-alkaline and A-type signatures took place at around 1.98-1.96 Ga, mainly to the north of the main belt, forming the Orocaima Igneous Belt (OIB) or a SLIP (Teixeira et al. 2019). South of the CCB, the Rio Urubu Igneous Belt (RUIB) encompasses 1.96-1.93 Ga A-type and High-K calc-alkaline granitoids and charnockite bodies showing complex structural pattern, interpreted as syn-kinematically emplaced during post-collisional transpression to the south of the CCB. Further west the Parima volcano-sedimentary basin was developed in response to the post-collisional tectonism. During the 1.89-1.87 Ga interval the Uatumã SLIP (Klein et al. 2012) obliterated the south-central part of the Guiana Shield (Fig. 1b).

The study area is located at the central portion of the Roraima State (Fig. 1c), where the Mucajaí Anorthosite-Mangerite-rapakivi Granite (AMG) Complex is exposed some kilometers to the south of the CCB (Fraga et al., 2009a; Heinonen et al., 2012). The AMG complex is surrounded by the Orosirian orthogneissic, and foliated granitic and charnockitic rocks from the Rio Urubu Igneous Belt.

The Mucajaí AMG Complex consists of rapakivi granites, mangerites, syenites and the Repartimento Anorthosite that forms a large igneous complex with remarkable asymmetrical compositional zoning and is considered as a rare manifestation of Mesoproterozoic intraplate magmatism in the northern Amazonian Craton (Heinonen et al., 2012; Teixeira et al. 2019). The Mucajaí rocks are well-dated. Gaudette et al. (1996) reported the age of 1544 ± 42 Ma (conventional method, U-Pb) for rapakivi granites. Santos et al. (1999) determined the age of 1527 ± 7 Ma (U-Pb, SHRIMP baddeleyite) for the Repartimento Anorthosite. Quartz Mangerites were dated at 1564 ± 21 Ma (Pb-Pb) and 1538 ± 5 Ma (Pb-Pb) by Fraga et al. (1997) and Fraga et al. (2009a), respectively. Recently, Heinonen et al. (2012) determined an U-Pb mean age of 1526 ± 2 for a Repartimento anorthosite, and U-Pb mean ages of 1526 ± 2 for a Mucajaí monzonite, 1527 ± 2 Ma for a Mucajaí hornblende granite, and a slightly younger age of 1519 ± 2 Ma for a Mucajaí biotite granite, all of them interpreted as the best estimate for the rock crystallization age. All these ages give a mean age of 1535.0 ± 7.5 Ma for the Mucajaí Complex.

To the northeast of the Mucajaí area, the Serra Grande Mountain was initially mapped as part of the Mucajaí complex (Reis et al., 2004). However, U-Pb dating on magmatic zircons of charnockitic and rapakivi granitic rocks from the mountain yielded ages of 1430 ± 3 Ma, 1431 ± 8 Ma, 1428 ± 5 Ma, 1425 ± 6 Ma and 1434 ± 11 Ma, demonstrating these rocks are ca. 100 Ma younger than rocks from the Mucajaí Complex (Santos et al., 2011).

Pegmatitic veins and xenoliths are not common in the Mucajaí rocks, and no evidence of metamorphism is observed (Fraga, 2002; Fraga et al., 2009a). However, ductile-brittle deformation developed at temperatures around 400°C producing mylonites associated to the 1200 Ma K'Mudku Episode, which affected the southern border of the complex (Fraga, 2002; Cordani et al., 2010). Reactivation of this mylonitic belt occurred during the opening of the Central Atlantic Ocean with installation of the Mesozoic Tacutu Graben (Fraga, 2002, Fraga and Costa, 2004). It is also worth mentioning the occurrence of two magmatic events related to the opening of the Tacutu basin: the NE-SW Taiano diabase dyke swarm in central Roraima State and the Tacutu rift Apoteri basalts (Reis et al., 2008). The Taiano dykes are from the Jurassic period as established by the Ar-Ar ages between 197.4 ± 1.9 Ma and 201.1 ± 0.7 Ma (Marzoli et al., 2004; Nomade et al. 2007), while the Apoteri basalts are c.a. 50 Ma younger as established by the Ar-Ar ages between 149.5 Ma e 153.5 Ma (Reis et al. 2008).

Journal Pre-proof

FIGURE 1

3. Sampling and methods

Paleomagnetic sampling was carried out in the area to the southwest of the Mucajaí town, close to Apiaú and Roxinho villages, at the central Roraima state, Brazil (Fig. 1c, Table 1). 139 oriented cylindrical cores (2.54 cm in diameter) were collected using a gasoline-powered drill from 22 sites of well-exposed outcrops represented by anorthosites (two sites), mangerites (eight sites) and rapakivi granites (12 sites) from the Mucajaí Complex. Samples were oriented using both sun and magnetic compasses. Trying to obtain a 1430 Ma paleomagnetic pole, 61 oriented cylindrical cores were also drilled from seven well-exposed sites from the Serra Grande Complex, composed by charnockites (one site), mangerites (two sites) and rapakivi granites (four sites).

At the laboratory, cylindrical cores were cut into 2.2 cm height specimens. Step-wise alternating magnetic field (AF) and thermal demagnetization techniques were employed to separate the characteristic remanent magnetization (ChRM) component. Steps of 2.5 mT (up to 15 mT) and 5 mT (15 mT-100 mT) were adopted for AF demagnetization using an AF demagnetizer coupled to a cryogenic superconducting magnetometer (2G-Enterprises), model 755-4K. Thermal demagnetization was performed using a TD-60 furnace of ASC Scientific in steps of 50°C (from 150°C up to 500°C) and 20°C (from 500°C up to 600°C). For samples with strong magnetization, the remanent magnetization measurements were carried out using a JR-6A spinner magnetometer (AGICO, Czech Republic). These instruments are housed in a magnetically-shielded room with ambient field < 1000 nT at the USPmag paleomagnetic laboratory of the University of São Paulo. Part of the samples were sent to Finland and analyzed at the Laboratory for Solid Earth Geophysics of the University of Helsinki. There, the following steps were used for AF demagnetization: Steps of 2.5 mT (up to 10 mT), steps of 5 mT (up to 30 mT), steps of 10 mT (up to 60 mT) and steps of 20 mT (up to 140 mT), and for thermal demagnetization, steps of 100, 150, 200, 300, 320, 400, 450, 500, 520, 540, 550, 560, 570, 575, 580°C.

Magnetic components for each specimen were identified in orthogonal plots (Zijderveld, 1967), and calculated using the Principal Component Analysis (Kirshvink,

Journal Pre-proof

1980). At least four successive demagnetization steps were used to calculate vectors using least-squares fits, and an upper limit for mean angular deviation (MAD) of 8° was applied. Fisher's (1953) statistics was used to calculate site mean directions and the paleomagnetic pole.

Magnetic mineralogy was investigated through the acquisition of isothermal remanent magnetization (IRM) using a pulse magnetizer MMPM10 (Magnetic Measurements), and with first-order-reversal-curves (FORC) and hysteresis curves using a MicroMag 3900 VSM (Princeton Measurements Corporation). These curves give bulk coercive force (H_c), coercivity of remanence (H_{cr}), saturation magnetization (M_s), and saturation remanent magnetization (M_{rs}), after subtraction of the paramagnetic contribution from the high field portion of the curve. To characterize the magnetic carriers in the samples, thermomagnetic curves (low-field magnetic susceptibility versus high and low temperature) were performed for several samples, using a CS-4 apparatus coupled with the KLY-4S Kappabridge instrument (AGICO, Czech Republic).

4. Magnetic Mineralogy

Normalized intensity curves (after AF treatment) show mean destructive fields (MDF) between 15 and 20 mT for most samples (e.g., samples FRM11-B1 (site 4), FRM22-F3 (site 15) and FRM23-E1 (site 16) in Fig. 2a), typical of titanomagnetite or magnetite. However, for other samples MDF is greater than 30 mT (e.g., sample FRM8-A4 (site 1) in Fig. 2a), and around 20% of the initial NRM remained at fields up to 100 mT, suggesting also the presence of other minerals, such as hematite.

Thermal demagnetization revealed distributed unblocking temperatures spectra for all samples (Fig. 2b). For most samples, significant intensity decay occurs between 520°/540°C and 580°/600°C, indicating the presence of Ti-poor titanomagnetite as the main magnetic carrier in the rock. However, a significant intensity decay also occurs at temperatures between 200°C and 350°/400°C for some samples, suggesting the additional presence of maghemite (e.g., samples FRM9-D3 (site 2), FRM13-B4 (site 6) and FRM26-B4 (site 19) in Fig. 2). For other samples the presence of hematite is also detected by the unblocking temperatures between 640°C and 700°C (e.g., samples FRM17-B4 (site 10) and FRM20-E3 (site 13) in Fig. 2).

Journal Pre-proof

FIGURE 2

Narrow-waisted hysteresis curves and saturation fields around 300 mT are observed in many samples, which is typical of low to moderate coercivity minerals as magnetite (Figs. 3a-d). Fig. 3e shows the Day's plot (Day et al., 1977, modified by Dunlop, 2002) indicating that most samples fall into the pseudo-single domain (PSD) grain size range or along a trend parallel to the theoretical single domain/multi-domain (SD/MD) mixing curves of Dunlop (2002). This behavior is consistent with the good magnetic stability obtained during AF and thermal treatments (see below). However, multi-domain (MD) magnetic grains exist in most samples and in several, they are dominant as shown by magnetic instability. Samples FRM22-F3 and FRM23-E1 (see Fig. 2) suggest that MD grains are dominant.

First order reversal curves (FORC) were obtained for selected samples to study the domain state indicated by the Day plot. FORC diagrams for an ensemble of SD-particles have the shape of a symmetrical distribution of the contour along the H_b axis, without a vertical scatter along the H_c axis, and for an ensemble of PSD particles they have an asymmetric distribution with a contour diverging along the vertical axis (Roberts et al., 2014). According to the FORC diagram (Figs. 4a-c), the magnetic minerals in the analyzed samples are in the SD or PSD state.

Irreversible high-temperature thermomagnetic curves were observed for practically all samples, most of them indicating that probably magnetite is formed during heating (Fig. 5). A pronounced Hopkinson peak, Curie temperatures near 580°C, and a well-characterized Verwey transition at around -153°C denoted by the low-temperature thermomagnetic curves are observed for most samples (Figs. 5b, c and d). These characteristic features are typical of thermally stable, SD/PSD Ti-poor titanomagnetite grains (Dunlop and Özdemir, 1997). During heating, some samples show inflexions on the susceptibility curves at temperatures around 350-400°C suggesting the presence of maghemite or Ti-rich titanomagnetite as a secondary mineral in these samples (Fig. 5c). Also, decreasing susceptibility up to 700°C in the high-temperature thermomagnetic curve (Fig. 5d), or the presence of the Morin transition at -15°C in low-temperature thermomagnetic curve (Fig. 5a) observed for

Journal Pre-proof

some samples, indicate that hematite is also present in these rocks. Finally, some samples show typical curves where paramagnetic minerals predominate (Figs. 5e and 5f). Susceptibility in these curves does not fall to zero at temperatures up to 700°C during heating, also suggesting the presence of hematite in these rocks.

For several samples, isothermal remanent magnetization (IRM) acquisition curves show practically identical behaviour, reaching saturation in fields below 300 mT, indicating a distribution of low coercivity grains such as magnetite or Ti-poor titanomagnetite (Fig. 6). Some samples (FRM8-E), however, reach saturation in fields higher than 300 mT indicating the presence of other minerals in these rocks, probably represented by hematite, as indicated above. For those samples AF demagnetization treatment (FRM8-A4, Fig. 2) was less efficient.

FIGURE 3

FIGURE 4

FIGURE 5

FIGURE 6

5. Paleomagnetic Results

The NRM intensities range from 809x10^{-6}A/m up to values as high as 101 A/m, due to lithological variations. High NRM values are obtained for anorthosites and mangerites samples and low NRM values for rapakivi granite samples. A summary of paleomagnetic results is given in Table 1. Samples from three sites (FRM10 – a biotite-hornblende granite, FRM25 – a mangerite, FRM28 – a rapakivi granite) yielded inconsistent and/or unstable behavior and will not be considered hereafter.

In general, secondary low coercivity or low unblocking temperature components were removed with AF fields $\leq$ 15-30 mT or temperatures $\leq$ 400°C. After removing secondary components, northwestern directions with upward inclinations or southeastern directions with downward inclination were disclosed (Figs. 7a - 7d). This characteristic remanent magnetization (ChRM) component (named as component A) was isolated in samples of 12 sites (Fig. 8a, Table 1) from the Mucajaí AMG Complex. Similar ChRM directions were also obtained for other three sites (one anorthosite and two biotite-granites) from the Mucajaí Complex by Veikkolainen et al. (2011), and are added to our data to give a more robust estimate of the dual polarity component A: Dm = 132.2°, Im = 35.4° (α_{95} = 12.7°, k = 10.0, N = 15, Table 1), which yield a paleomagnetic pole (MC-A) at 0.1°E, 38.2°S (A_{95}=12.6°, K=10.2).

AF and thermal demagnetization performed for the remaining seven sites (FRM8, FRM11, FRM13, FRM14, FRM15, FRM27, FRM29*)* revealed dual polarity (northeastern/southwestern) directions with low to moderate inclinations (Figs. 7e, 7f*)*, here labeled as component B. The corresponding site mean directions (Fig. 8b) cluster around the mean, Dm = 50.3 °, Im = 3.8 °, (α_{95} = 23.6°, k = 7.5, N = 7 sites), which yield a paleomagnetic pole (MC- B) at 207.7°E, 39.8°S (A_{95} = 14.6°; K=18.1) (Table 1).

Samples from four out the seven analyzed sites from the Serra Grande Suite yielded only the component B (Fig. 9). Samples from the other three sites (FRM1, FRM3, FRM7) showed unstable or inconsistent results. Site mean directions calculated for these four stable sites are presented in Table 1. A combined mean direction for component B using the seven sites from the Mucajaí Complex and the four sites from the Serra Grande Complex, reveal Dm = 47.3°, Im = -2.7°, α_{95} = 17.5°, k = 7.8, corresponding to a paleomagnetic pole at 212.7°E, 42.6°S (A_{95} = 11.0°; K=18.0) (MC/SG-B pole, Table 1).

TABLE 1

FIGURE 7

FIGURE 8

FIGURE 9

6. Discussion

6.1. The age of component B

The dual polarity component B was disclosed for 94 samples from seven sites of the Mucajaí complex (~ 1535 Ma), and for 36 samples from four sites of the Serra Grande complex (~ 1430 Ma). This component is characterized by different unblocking temperatures between (520°-540°C and 580°-600°C) and (200°C and 350°-400°C), suggesting that magnetization is carried by titanomagnetite and maghemite minerals. Several scenarios for the origin of component B can be presented. First, a possible interpretation is that the Serra Grande magmatism would have thermally affected part of the rocks from the Mucajaí complex and remagnetized them at 1430 Ma. In this case, component B would be of primary origin in the Serra Grande Suite, and secondary in Mucajaí complex. However, as already stressed, the Serra Grande complex rocks were affected by the opening of the Mesozoic Tacutu graben, which cut across the Serra Grande rocks. Basaltic magmatism is associated with the Tacutu rift which is not genetically related to the NE-SW and E-W Taiano diabase dyke swarm (Reis et al., 2003, 2006). Ar-Ar geochronology yielded ages between 197.4 ± 1.9 Ga and 201.1 ± 0.7 Ma for the dykes (Marzoli et al., 1999) while a younger age was attributed to the Apoteri basalts (Reis et al., 2006). The MC/SG-B pole (component B) is overlapping with the Mesozoic "197 Ma pole" that defines the Mesozoic (215-170 Ma) apparent polar wander path for South America (Llanos and Prezzi, 2013) (Fig. 10a). This suggests that component B (MC/SG-B pole), most probably, represents a remagnetization occurred during the Taiano dyke intrusions, and the related Central Atlantic magmatic province (CAMP) activity.

FIGURE 10

Journal Pre-proof

6.2. The age of component A

Component A was separated for 160 samples from 12 sites of the Mucajaí Complex, and it is carried by SD/PSD Ti-poor titanomagnetite/magnetite and/or hematite. Combined with results from other three sites previously published (Veikkolainen et al., 2011) a mean direction was calculated Dm = 132.2°, Im = 35.4° (α_{95} = 12.7°, k = 10.0, N = 15), yielding a paleomagnetic pole (MC-A pole) at 0.1°E, 38.2°S (A_{95}=12.6°; K=10.2) (Table 1). This pole differs significantly from the South American Mesozoic and Cenozoic poles indicating that component A does not represent a recent remagnetization (Llanos and Prezzi, 2013). Also, it does not coincide with any part of the Paleozoic apparent polar wander path traced for Gondwana (Torsvik et al., 2012, see their Fig. 12b).

On the other hand, the southern part of the Mucajaí complex was affected by the ~1200 Ma K'Mudku tectonic event. This region is characterized by a narrow belt of shear zones, which produced mylonitization in a brittle-ductile condition of local granitic rocks (Santos et al., 2000; Fraga et al., 2009a, b; Cordani et al., 2010).

Concerning ~1200 Ma (K'Mudku episode) paleomagnetic data within Amazonia, there is only the Nova Floresta Formation (ca. 1400 km to the south of Mucajaí) pole (NFF, Plat = 24.6°N, Plong = 164.6°E, A_{95}=5.5°), dated at 1198 ± 3 Ma (Ar-Ar in biotite) (Tohver et al., 2002). Comparison of pole NFF with the MC-A Mucajaí pole (Fig. 10b) suggests that they are different (their confidence circles did not overlap). On the other hand, the MC-A pole overlaps the coeval pole of the 1540 Ma Parguaza rocks (Valdespino and Costanzo-Alvarez, 1997) (Fig. 10b). The Parguaza batholith is composed of rapakivi granites and represents the latest magmatic event of the Cuchivero Province in Venezuela (Gaudette et al., 1978). The absence of epidote and chlorite, and no visible alteration and metamorphism are evidence that the original ferromagnetic minerals are still present in the rocks, a prerequisite for primary magnetization. Besides, the magnetic mineralogy analysis identified SD magnetite as a primary carrier in the Parguaza rocks (Valdespino and Costanzo-Alvarez, 1997).

The Mucajaí MC-A pole (0.1°E, 38.2°S, A_{95}=12.6°, K=10.2) satisfies six out of the seven quality criteria proposed by Van der Voo (1990) and Buchan et al. (2000):

(i) U-Pb dating on rocks of the AMG Complex provided an average age of 1535.0 ± 7.5 Ma (see above). Some of the sampled sites for paleomagnetic analysis are the same that were radiometrically dated [1538 ± 5 Ma (Pb-Pb); 1527 ± 7 Ma (U-Pb, SHRIMP); 1544 ± 42 Ma (conventional method, U-Pb), 1526 ± 2 Ma (U-Pb), 1527±2 Ma (U-Pb) and 1519±2 Ma (U-Pb) by Fraga (2002); Fraga et al. (2009b); Santos et al. (1999); Gaudette et al. (1996); and Heinonen et al. (2012)]. Unfortunately, no Ar-Ar radiometric data are available for these rocks to estimate the cooling rate of the Mucajaí Complex, and then establish the age of the MC-A pole. Valdespino and Costanzo-Alvarez (1997) suggest a much younger age (1440 Ma) for their G1 component from which the Parguaza pole was calculated (Table 2), based on Rb-Sr model ages (Chrontours map – see their Fig. 3). However, the Parguaza pole is very different from the 1440-1420 Ma Amazonian poles, represented by the Salto do Céu (1440 Ma), Rio Branco sedimentary rocks, Nova Guarita dykes (1420 Ma) and Indiavaí

Intrusive (1416 Ma) (D'Agrella-Filho et al., 2016a, b). Also, an initial fast cooling of the Parguaza and Mucajaí rocks cannot be discarded. A thermochronometric study (Ar-Ar data) of the Imataca metamorphic Complex (in northern Venezuela) shows a relatively initial fast cooling (up to 350°-400°C) of the complex at about 1950-1930 Ma (Onstott et al., 1989, see their Fig. 15). The same could have happened with the Parguaza and Mucajaí Complexes. SD/PSD magnetite grains with high unblocking temperatures (> 520°-540°C) are the main magnetic carriers of the characteristic remanent magnetization of these rocks. A remanent magnetization carried by magnetite grains with such high blocking temperatures would have been survived even if the rocks remained for hundreds of millions of years at 400°C (Pullaiah et al., 1975). In view of the absence of a thermochronometric study of the investigated Mucajaí Complex we understand that the best estimate of the MC-A pole is the mean of all available U-Pb ages, that is, 1535 ± 8 Ma;

(ii) 160 out 234 analyzed specimens from 12 sites were used to determine component A. This component was also observed in previous analysis of the Mucajaí Complex for 17 samples of three sites (Veikkolainen et al., 2011). The combined results yielded the MC-A paleomagnetic pole which shows a*dequate Fisher's statistical* parameters (A_{95}<16° and K>10.0) according to the second criterion of Van der Voo (1990). Also, the semi-angle cone of confidence (A_{95}=12.6°) calculated for the Mucajaí pole falls in the expected interval of ~ 4° to 15° predicted in the secular variation models (Deenen et al., 2011). Moreover, the number of sites (15) used to calculate the Mucajaí pole is considered the minimum necessary to eliminate secular variation by these authors. On the other hand, the precision parameter (K=10.2) of the Mucajaí pole implies an angular dispersion (s) of 25.4° for the paleolatitude (λ) of 19.6° calculated using the Mucajaí mean magnetic inclination Im=35.4°. Proterozoic models of secular variation, however, predicts a much lower value for s, of ca. 12° to 13°, for a paleolatitude of ~20° (Smirnov et al., 2011, Veikkolainen and Pesonen, 2014). As was speculated by Kirscher et al. (2019), high angular dispersions (associated to low K values) for Paleo- to Mesoproterozoic (1800-1500 Ma) poles may be related to the low geomagnetic dipole field intensity at that time (see Smirnov, 2017, Biggin et al., 2015), when the relatively enhanced non-dipole field produced an increased dispersion of directions. On the other hand, radiometric ages between 1544 and 1519 Ma (see

Journal Pre-proof

Journal Pre-proof

above) suggest a protracted life of the Mucajaí Complex, which alternatively may also be responsible for the poor grouping of the site mean directions, and consequently the inconsistent high angular dispersion (s);

(iii) ChRM components were isolated by least-squares fit from orthogonal diagrams (Kirschvink, 1980) after AF and thermal demagnetization;

(iv) Unfortunately, a magnetic stability test (*baked contact test*) could not be performed to ascertain the primary nature of component A because exposure of the contact aureole zone was not found;

(v) The studied rocks are not deformed or metamorphosed (Gaudette et al., 1996). Also, the Mucajaí AMG Complex is considered as an intracratonic event located in the northern part of the Amazonian Craton (Guiana Shield) which was tectonically stable after intrusion. Moreover, similar directions were disclosed for the tectonically preserved ca. 1545 Ma Parguaza rocks in Venezuela (see discussion above) demonstrating that no significant relative tilting or rotation occurred between these areas;

(vi) Both polarities were observed in the analyzed sites, attesting that a long time elapsed during intrusion of the magmatic rocks of the Mucajaí AMG Complex, probably enough to eliminate the secular variation of the geomagnetic field. The McFadden and McElhinny (1990) reversal test was applied in the component A directions and the following parameters were determined: critical angle (γ_c = 38.2°) and observed angle (γ_o = 168.8°). These parameters classify the reversal test as 'undetermined', since $\gamma_o > \gamma_c$ and $\gamma_c > 20°$. Thus, this test does not ensure that secondary components were completely eliminated from the isolated characteristic remanent magnetization after AF and thermal treatments. However, the very small number of Mucajaí sites with upward direction (only 2, Table 1) may have influenced in the results of the reversal test;

(vii) As already stressed, two tectonic events (the ca. 1200 Ma K'Mudku shear event and the ca. 200 Ma Tacutu graben event) partially affected the Mucajaí rocks, which could imprint a secondary remanence in the rocks. However, pole MC-A is very different from the Phanerozoic poles, and although lies close to the 1200 Ma Nova Floresta pole, it is statistically (95%) different from that. Moreover, the confidence circles (A95) of the MC-A and Parguaza poles overlap suggesting similar ages for these two poles (Valdespino and Costanzo-Alvarez, 1997; Table 2).

Thus, the Mucajaí paleomagnetic pole can be considered as a robust paleomagnetic pole (Q=6) according to the quality criteria of Van der Voo (1990) and can be used to infer the paleogeographic position of the Amazonian Craton around 1530 Ma.

6.3. *Palaeogeography of the Amazonian Craton in Columbia supercontinent at 1530 Ma*

In recent years, paleomagnetic data have significantly contributed to test geological models that establish the participation of the Amazonian Craton in the Columbia supercontinent (e.g., Reis et al., 2013; Bispo-Santos et al., 2008, 2012, 2014a, 2014b; D'Agrella-Filho et al., 2012, 2016a).

For example, the SAMBA (South America - BAltica) model, which is based on geological correlations (or matchings) proposes that present northwestern Amazonian Craton was linked to present southwestern Baltica continent along Paleo-to Mesoproterozoic mobile belts (Johansson, 2009). In this model West Africa was linked to Amazonian Craton (Gondwana configuration), and to southeastern Baltica. Besides, northeastern Laurentia (along Greenland) was attached to northwestern Baltica along the coast of northern Norway. According to Johansson (2009) this great landmass formed the core of Columbia and persisted by ca. 500 Ma from 1800 Ma to 1300 Ma. The Baltica–Laurentia link has received considerable support from several paleomagnetic data sets, although the exact position of Baltica relative to Laurentia has various options (Buchan et al., 2000; Salminen and Pesonen, 2007; Evans and Pisarevsky, 2008; Hamilton and Buchan, 2010; Lubnina et al., 2010; Pisarevsky and Bylund, 2010; Salminen et al., 2009, 2014, 2016a, 2016b, 2017). The Baltica-Laurentia link was successfully tested at several times between 1830 and 1270 Ma, suggesting a longevity connection between these continents (e.g., Buchan et al., 2000; Pesonen et al., 2012; Cawood and Pisarevsky, 2017).

The Amazonia-Baltica link in SAMBA model was firstly tested by the paleomagnetic study of the well-dated 1789 Ma Avanavero rocks, representing a Large Igneous Province (LIP) located in the State of Roraima (Guiana Shield) (Reis et al., 2013;

Bispo-Santos et al., 2014a). A robust pole was obtained for these rocks, which supports a SAMBA-like model, suggesting that a great continental mass comprised of West Africa, Amazonia, Baltica, and Laurentia was already amalgamated at ca. 1780 Ma, forming the core of Columbia supercontinent (Bispo-Santos et al., 2014a). However, a contrasting interpretation was presented by Pisarevsky et al. (2014). These authors suggest that Columbia Supercontinent began its amalgamation somewhat later, at ca. 1700 Ma, reaching its maximum packing between 1650-1580 Ma, and notably, that the Amazonian Craton (together with West Africa Craton) did not participate in this supercontinent.

Given these controversial scenarios, the new 1530 Ma Mucajaí pole presented here for the Amazonian Craton can be used to test again the SAMBA model for such age. The paleogeography of the Columbia's core at around 1530-1540 Ma (Fig. 11a) was reconstructed using the following Euler poles: Laurentia (38.4°N, 280.4°E, -117.4°), Baltica (42.98°N, 243.9°E, -96.75°) and Amazonian Craton (9.28°N, 75.8°E, 32.5°) (see Table 2). The Laurentia/Baltica link in Fig. 11a is the same to that proposed by Evans and Pisarevsky (2008). The Baltica/Amazonia link, however, follows the SAMBA model but not exactly in the same configuration as proposed by Johansson (2009), whose Euler pole was calculated by Zhang et al. (2012).

TABLE 2

FIGURE 11

Selected paleomagnetic poles between 1800 Ma and 1400 Ma are presented in Table 2 for Amazonia, Baltica and Laurentia. For the Amazonian Craton, two paleomagnetic poles are available with ages around 1530-1550 Ma: (i) The Parguaza batholith pole (Valdespino and Costanzo-Alvarez, 1997) with an age of 1545 ± 20 Ma (U-Pb, zircon); and (ii) the 1535 Ma Mucajaí Complex pole of this work.

For Baltica, three paleopoles were selected with quality factor Q≥3 (Van der Voo, 1990) and ages between 1580Ma to 1540 Ma: (i) the key paleopole determined for the well-dated 1575 ± 3 (U-Pb) Åland Archipelago intrusive rocks in Finland (Salminen et al., 2016a); (ii) the key paleopole obtained for the well-dated 1576 ± 3 Ma

(U-Pb) Satakunta dikes of Finland (Salminen et al., 2014); and (iii) paleopole obtained for the Dala sandstones (Sweden) whose age of ~ 1540 Ma was inferred from the apparent polar wander (APW) path of Baltica (Piper and Smith, 1980) A combined grand mean was calculated for these poles due to their similar geographical positions (Table 2).

There are no paleomagnetic data in the time span of 1550-1530 Ma for Laurentia. Considering the interval between 1600 Ma and 1520 Ma, only the well-dated 1590 ± 3 (U-Pb) Western Channel dykes pole is available (Hamilton and Buchan, 2010).

These 1590 to 1530 Ma selected paleopoles for Amazonia, Baltica and Laurentia, after rotating them with the Euler poles assigned to their respective continental blocks (listed in Table 2), are well-grouped (see Fig. 11b). This also suggests that the continental blocks that composed the core of Columbia stayed practically stationary between 1590 Ma and 1530 Ma. Although different scenarios can be envisaged for the Amazonian Craton due to polarity ambiguity (Pisarevsky et al., 2014) the fact that a SAMBA-like model can be supported by paleomagnetic data at two different ages (1780 Ma and 1540 Ma) reinforces the idea that Baltica and Amazonia were part of the same continental mass, and that subduction-related Paleo- to Mesoproterozoic mobile belts developed in its western part (Fig. 11a) (see Pesonen et al., 2003; 2012).

A similar paleogeographic configuration was also proposed by Salminen et al. (2016a) at 1590 Ma based on paleomagnetic data. These authors suggest that Laurentia, Siberia, Baltica, and Amazonia/West Africa formed the nucleus of Columbia and occupied low to moderate latitudes at 1590 Ma.

6.4. *SAMBA connection longevity on the Columbia Supercontinent*

The Mucajaí Complex MC-A pole permits to reconstruct the Amazonian Craton in the configuration of the Columbia Supercontinent at 1540-1530 Ma (Fig. 11). This configuration shows Amazonia linked to Baltica in the SAMBA-like model of Johansson (2009). One aim is to test when Amazonia broke apart from Columbia and perhaps drifted independently to collide again with Laurentia during the assembly of the Rodinia supercontinent with other partners such as Baltica and West Africa. For this test we selected paleomagnetic poles in the interval between 1780 Ma and 1400 Ma (Table 2) for Laurentia, Baltica and Amazonia. These poles were rotated using the Euler rotation poles (Table 2) used in the configuration of the core of Columbia (Fig. 11, Fig 12).

By far the best results are from Baltica for which, key paleomagnetic poles are available for five periods in this time interval, at 1780 Ma, 1700 Ma, 1640 Ma, 1570 Ma and 1460 Ma (e.g. Salminen et al., 2017, Elming et al., 2019). At 1770-1790 Ma, Baltica is represented by the (i) 1770 ± 12 Ma (U-Pb) Propruchey sills pole, interpreted as representing a primary magnetization (Fedotova et al., 1999), (ii) the 1786 ± 10 Ma (U-Pb) Hoting gabbro, also interpreted as representing a primary origin (Elming et al., 2009), (iii) the 1785-1770 Ma (U-Pb on zircon) Småland mafic intrusions pole (Pisarevsky and Bylund, 2010), and the (iv) Shosksha Formation pole, whose sedimentation age is considered to be between 1790 and 1770 Ma (Pisarevsky and Sokolov, 2001). A combined mean pole was calculated for these four poles (pole BA1 in Table 2) which represents the Baltica mean pole at 1780 Ma.

Recently, Elming et al. (2019) published paleomagnetic and geochronological results for the Turinge gabbros (Sweden). A positive baked contact test, and ages around 1700 Ma, allowed the authors to characterize the Turinge gabbros pole (BA2 in Table 2) as a key pole representing Baltica at 1700 Ma. A key pole (BA3 in Table 2) was also obtained for the 1642 ± 2 Ma Häme diabase dykes (Salminen et al., 2017) with a maximum quality factor Q=7 (Van der Voo, 1990).

As already pointed out above key poles were also obtained for the 1576 ± 3 Ma Åland dykes (Salminen et al., 2016a) and the 1576 ± 3 Ma Satakunta dyke swarm (Salminen et al., 2014). The former includes the data of the 1540 ± 12 Ma Föglö-Sottunga dykes (Pesonen and Neuvonen, 1981). Including the ca. 1540 Ma Dala Sandstones pole with Q=4 (Piper and Smith 1980), we calculated a combined mean pole (BA6 in Table 1) to represent Baltica at ca. 1550 Ma.

A key pole was determined for the well-dated (U-Pb, baddeleyite) 1457 ± 2 Ma Lake Ladoga mafic rocks (Salminen and Pesonen, 2007; Lubnina et al., 2010). Other coeval poles were obtained for the 1469 ± 9 Ma Bunkris-Glysjön-Öje dykes (Bylund, 1985; Pisarevsky et al., 2014), the Salmi Formation at 1460 Ma (Shcherbakova et al., 2006), the Tuna dykes dated between 1461-1462 Ma (Bylund, 1985), and the 1458 $^{+4}/_{-}$

Journal Pre-proof

$_{3}$ Ma Valaam sills (Salminen and Pesonen, 2007). A combined mean pole was calculated for these five poles which represents Baltica mean pole at ca. 1460 Ma (BA8 in Table 2). Other selected paleopole was obtained for the Oskarhamn-Alsterbo dolerites aged around 1430 Ma (BA9 in Table 2).

These paleomagnetic poles define an apparent polar wander (APW) path for Baltica between 1780 Ma and 1430 Ma, as also suggested by Salminen et al. (2017) including a quasi-static position of Baltica between 1780 Ma and 1700 Ma (Elming et al., 2019). Paleomagnetic poles from Amazonia and Laurentia for this time interval (Fig. 12, Table 2) fall along the Baltica APW path, after rotating them using Euler poles presented in Table 2. At ca. 1780 Ma the LA1 (Laurentia), CA1 (Amazonia Craton) and BA1 (Baltica) poles are closely grouped corroborating the paleogeography presented in Fig. 11, which was also positively tested by the 1540 Ma Mucajaí pole (see above). The combined (CA2) mean pole obtained for the la Escalera, Rio Aro and Guyana dolerites falls around the 1700 Ma Baltica APW path. Although this pole was defined for 18 sites (Onstott et al., 1984) collected at very different areas, its age (1640 Ma – Rb-Sr isocron) is not yet well-constrained, and new ages using more precise geochronological methods (U-Pb on baddeleyites or Ar-Ar) are needed.

Between 1640 Ma and 1540 Ma, paleomagnetic poles from Baltica and Laurentia apparently define only a minor polar drift (Fig. 12). This suggests another quasi-static position of this continental mass. The 1440 Ma Salto do Céu sills pole (CA6) and Rio Branco sedimentary rocks pole (CA5) from Amazonia statistically coincide with the 1430 Ma Oskarhamn-Alsterbo dolerites pole (BA9) from Baltica. However, the Nova Guarita pole (CA7) and the Indiavaí pole (CA8) seem to define a different polar trajectory for Amazonia compared to that defined for Laurentia and Baltica (Fig. 12). A possible interpretation is that Columbia supercontinent began to break-up at about 1440-1420 Ma (Bispo-Santos et al., 2012). Another possible interpretation is that internal relative rotations of these cratonic blocks occurred within Columbia supercontinent, at some time between 1540 Ma and 1440 Ma (D'Agrella-Filho et al., 2016a, b).

The available paleomagnetic data for Baltica, Laurentia and Amazonia suggest that the reconstruction proposed in Fig. 11 remained for a long time, from 1780 Ma up to 1440 Ma, at least. This configuration corroborates the model by Johansson (2009) that proposes that Laurentia, Baltica, Amazonia and West-Africa formed, in this sequence, a large continental mass (core of Columbia) at Paleo-Mesoproterozoic times, and subduction-related accretionary belts developed at its western side during such interval (Pesonen et al., 2003, 2012; Salminen et al., 2016a).

This long life core of Columbia has also been proposed by other authors, which included other cratonic blocks, like Siberia, North China, India and proto-Australia (e.g., Evans and Mitchell, 2011; Zhang et al., 2012; Xu et al., 2014). The strong decrease in the subduction related magmatism that prevailed in the Mesoproterozoic is consistent with a long life Columbia (Silver and Behn, 2008). Continental blocks that formed Columbia show evidence of intense intracratonic magmatic activity represented by voluminous anorogenic rapakivi granitic intrusions and associated anorthosite, mangerite and charnockite rocks (AMCG complex) between 1600 and 1300 Ma, from which the Mucajaí magmatic AMG Complex in Amazonian Craton is an example (e.g., Åhäll and Connelly, 1998; Bettencourt et al., 1999; Emslie et al., 1994; Rämö and Haapala, 2005; Rämö et al., 2003; Heinonen et al., 2012; Pesonen et al.,2012). Vigneresse (2005) argues that high temperatures (1300°C) at the base of the crust are necessary for intrusion of these magmatic rocks. These temperatures would be reached in a long time (over 200 Ma) by heat diffusion and melting over descending lithospheres after agglutination of the Columbia supercontinent, which would stay quasi-stationary along this time. Interestingly, Fig. 12 indeed shows a low APW path drift rate between 1780 Ma and 1560 Ma (ca. 220 Ma) with the first AMCG complexes being intruded at ca. 1600 Ma.

FIGURE 12

7. Conclusions

Paleomagnetic analysis was performed on rocks from the 1535 Ma (U–Pb, zircon) Mucajaí AMG Complex, northern Amazonian Craton (Roraima State, Brazil). AF and thermal treatments revealed northwestern/southeastern directions with upward/downward inclinations (component A), carried by high-coercivity and high blocking-temperature Ti-poor titanomagnetite grains. The calculated mean direction (Dm=132.2°; Im=35.4°, N=15; α_{95}=12.7°) for the Mucajaí Complex rocks yielded a paleomagnetic pole (MC-A pole) located at 0.1°E, 38.2°S (A_{95}=12.6°), which can be classified with a reliability factor Q = 6. The presently available 1780 to 1440 Ma paleomagnetic data corroborate the SAMBA model of Johansson (2009), where proto-Amazonia/West Africa was linked to Baltica, and Baltica to Laurentia, in the Columbia Supercontinent. This long life continental mass may have broken-up at 1440 Ma (Bispo-Santos et al., 2012) or, alternatively, integrity of Columbia was preserved by a longer time, but Amazonia/West Africa rotated relative to Baltica/Laurentia at some time between 1540 and 1420 Ma ago (D'Agrella-Filho et al., 2016a, b). Paleomagnetic data also suggest a quasi-stationary Columbia supercontinent between 1780 Ma and 1540 Ma, which resulted in the occurrence of the incratonic 1600 Ma to 1400 Ma AMCG complexes, well-characterized in Baltica, Amazonia and Laurentia (Vigneresse, 2005).

Acknowledgments

We thank CNPq research fellowships to Franklin Bispo dos Santos (PDJ -150649/2017-7) and M. S. D'Agrella Filho (303130/2014-8), FAPESP grant (2016/13689-5) for financial support and the Geological Survey of Brazil (CPRM – Manaus) for its help in field work logistics. Johanna Salminen was funded by Academy of Finland. We also thank the valuable comments of the reviewers that greatly improved the manuscript.

References

Åhäll, K.-I., Connelly, J., 1998. Intermittent 1.53-1.13 Ga magmatism in Western Baltica; age constraints and correlations within a postulated supercontinent. *Precambrian Research* 92, 1-20.

Almeida, F.F., Hasui, Y., Brito-Neves, B.B., Fuck, R.A., 1981. Brazilian structural provinces: an introduction. *Earth Science Review* 17, 1-19.

Bettencourt, J.S., Leite Jr., W.B., Ruiz, A.S., Matos, R., Payolla, B.L., Tosdal., R.M., 2010. The Rondonian-San-Ignacio Province in the SW Amazonian Craton: An overview. *Journal of South American Earth Sciences* 29, 28-46.

Bettencourt, J.S., Tosdal, R.M., Leite Jr., W.B., Payolla, B.L., 1999. Mesoproterozoic rapakivi granites of the Rondônia Tin Province, southwestern border of the Amazonian craton, Brazil - I. Reconnaissance U-Pb geochronology and regional implications. *Precambrian Research* 95, 41-67.

Biggin, A.J., Piispa, E.J., Pesonen, L.J., Holme, R., Paterson, G.A., Veikkolainen, T., Tauxe, L., 2015. Palaeomagnetic field intensity variations suggest Mesoproterozoic inner-core nucleation. *Nature* 526, 245–248.

Bispo-Santos, F., D'Agrella-Filho, M.S., Pacca, I.I.G., Janikian, L., Trindade, R.I.F., Elming, S.-Ǻ., Silva, J.A., Barros, M.A.S., Pinho, F.E.C. 2008. Columbia revisited: Paleomagnetic results from the 1790 Ma Colíder volcanics (SW Amazonian Craton, Brazil). *Precambrian Research* 164, 40-49.

Bispo-Santos, F., D'Agrella-Filho, M.S**.**, Trindade, R.I.F., Elming, S.A., Janikian, L., Vasconcelos, P.M., Perillo, B.M., Pacca, I.G., Silva, J.A., Barros, M.A.S. 2012. Tectonic implications of the 1419 Ma Nova Guarita mafic intrusives paleomagnetic pole (Amazonian Craton) on the longevity of Nuna. *Precambrian Research* 196-197, 1-22.

Bispo-Santos, F., D'Agrella-Filho, M.S., Trindade, R.I.F., Janikian, L., Reis, N.J. 2014a. Was there SAMBA in Columbia? Paleomagnetic evidence from 1790 Ma Avanavero mafic sills (Northern Amazonian craton). *Precambrian Research* 244, 139-155.

Bispo-Santos, F., D'Agrella-Filho, M.S., Janikian, L., Reis, N.J., Reis, M.A.A.A. Trindade, R.I.F. 2014b. Towards Columbia: Paleomagnetism of 1980–1960 Ma Surumu volcanic rocks, Northern Amazonian Craton. *Precambrian Research* 244, 123-138.

Buchan, K. L., Mertanen, S., Park, R. G. Pesonen, L. J., Elming, S. A., Abrahamsen, N., Bylund, G., 2000. Comparing the drift of Laurentia and Baltica in the Proterozoic: the importance of key palaeomagnetic poles. *Tectonophysics* 319, 167-198.

Bylund, G., 1985. Palaeomagnetism of middle Proterozoic basic intrusive in central Swedem and the Fennoscandian apparent polar wander path. *Precambrian Research* 28, 283-310.

Cawood, P.A., Pisarevsky, S.A., 2017. Laurentia-Baltica-Amazonia relations during Rodinia assembly. *Precambrian Research* 292, 386-397.

Cordani, U.G., Teixeira, W. 2007. Proterozoic accretionary belts in the Amazonian Craton. *Geological Society of America Memoir* 200, 297–320.

Cordani, U. G., Fraga, L, M., Reis, N., Tassinari, C. C. G., Brito-Neves, B. B. 2010. On the origin and tectonic significance of the intra-plate events of Grenvillian-type age in South America: A discussion. *Journal of South American Earth Sciences* 29, 143–159.

D'Agrella-Filho, M.S., Trindade, R.I.F., Elming, S.A., Teixeira, W., Yokoyama, E., Tohver, E., Geraldes, M.C., Pacca, I.I.G., Barros, M.A.S., Ruiz, A.S. 2012 The 1420 Ma Indiavaí Mafic Intrusion (SW Amazonian Craton): Paleomagnetic results and implications for the Columbia supercontinent. *Gondwana Research* 22, 956-973.

D'Agrella-Filho, M.S, Trindade, R.I.F., Queiroz, M.V.B., Meira, V.T., Janikian, L., Ruiz, A.S., Bispo-Santos, F., 2016a. Reassessment of Aguapeí (Salto do Céu) Paleomagnetic pole of the Amazonian Craton and implications for Proterozoic supercontinents. *Precambrian Research* 272, 1-17.

D'Agrella-Filho. M. S., Bispo-Santos, F., Trindade, R. I. F., Antonio, P.Y.J., 2016b. Paleomagnetism of the Amazonian Craton and its role in paleocontinents. *Brazilian Journal of Geology* 46, 275-299.

Dall'Agnol, R., Dreher, A.M., Araujo, J.F.V., Abreu, A.S., 1975. Granito Surucucu. Anais 10th Conferência Geológica Interguianas. *Departamento Nacional da Produção Mineral*, Belém, pp. 340-388.

Dall'Agnol, R., Costi, H.T., Leite, S.A.A., Magalhães, M.S., Teixeira, N.P., 1999. Rapakivi granites from Brazil and adjacent areas. *Precambrian Research* 95, 9-39.

Day, R., Fuller, M., Schmidt, V. A., 1977. Hysteresis properties of titanomagnetites: Grain size and composition dependence. *Physics of the Earth Planetary Interiors* 13, 260–267.

Deenen, M.H.L., Langereis, C.G., van Hinsbergen, D.J.J., Biggin, A.J., 2011. Geomagnetic secular variation of palaeomagnetic directions. *Geophysical Journal International* 186, 509-520.

Dunlop, D.J., 2002. Theory and application of the Day plot (Mrs/Ms versus Hcr/Hc) 1. Theoretical curves and tests using titanomagnetite data. *Journal of Geophysical Research* 107, B3, 10.1029/2001JB000486, 4-1 - 4-22.

Dunlop, D.J., Özdemir, Ö., 1997. Rock Magnetism, Fundamentals and Frontiers. *Cambridge University Press*, Cambridge, 573.

Elming, S.Å., Moakhar, M.O., Layer, P., Donadini, F., 2009. Uplift deduced from remanent magnetization of a proterozoic basic dyke and the baked country rock in the Hoting area, Central Sweden: a palaeomagnetic and ^{40}Ar/^{39}Ar study. *Geophysical Journal International* 179, 59–78.

Elming, S.-Å., Pesonen, L.J., 2010. Recent Developments in Paleomagnetism and Geomagnetism. *Sixth Nordic Paleomagnetic Workshop*, Luleå (Sweden), 15–22 September 2009. EOS, vol. 90 (51), pp. 502.

Elming, S.-Å., Layer, P., Söderlund, U., 2019. Cooling history and age of magnetization of a deep intrusion: A new 1.7 Ga key pole and Svecofennian-post Svecofennian APWP for Baltica. *Precambrian Research* 329, 182-194.

Elston, D.P., Bressler, S.L., 1980. Paleomagnetic poles and polarity zonation from the Middle Proterozoic Belt Supergroup, Montana and Idaho. *Journal of Geophysical Research* 85, 339-355.

Elston, D.P., Enkin, R.J., Baker, J., Kisilevsky, D.K., 2002. Tightening the Belt: Paleomagnetic-stratigraphic constraints on deposition, correlation, and deformation of the Middle Proterozoic (ca. 1.4 Ga) Belt-Purcell Supergroup, United States and Canada. *Geological Society of American Bulletin* 114, 619–638.

Emslie, R.F., Irving, E., Park, J.K., 1976. Further paleomagnetic results from the Michikamau Intrusion Labrador. *Canadian Journal of Earth Sciences* 13, 1052–1057.

Emslie, R.F., Hamilton, M.A., Thériautl, R.J., 1994. Petrogenisis of a Mid-Proterozoic anorthosite-mangerite-charnockite-granite (AMCG) complex: isotope and chemical evidence from the Nain Plutonic suite. *Journal of Geology* 102, 539-558.

Evans, D. A. D., 2013. Reconstructin pre-Pangean supercontinents. *Geological Society of American Bulletin* 125, 1735-1751.

Evans, D.A.D., Mitchell, R. N. 2011. Assembly and breakup of the core of Paleoproterozoic–Mesoproterozoic supercontinent Nuna. *Geology* 39, 443–446.

Evans, D.A.D., Pisarevsky, S.A., 2008. Plate tectonics on early Earth? Weighing the paleomagnetic evidence. In: Condie, K.C., Pease, V. (eds.), When Did Plate Tectonics Begin on Planet Earth? *Geological Society American Special Paper* 440, 249–263.

Fedotova, M.A., Khramov, N.A., Pisakin, B.N., Priyatkin, A.A., 1999. Early Proterozoic palaeomagnetism: new results from the intrusives and related rocks of the Karelian, Belomorian and Kola provinces, eastern Fennoscandian Shield. *Geophysical Journal International* 137, 691–712.

Fisher, R.A., 1953. Dispersion on a sphere. Proceedings of the Royal Society of London 217, 295–305.

Fraga, L.M., 2002. A Associação Anortosito – Mangerito – Granito Rapakivi (AMG) do Cinturão Guiana Central e suas Encaixantes Paleoproterozóicas: Evolução Estrutural, Geocronologia e Petrologia. Tese de Doutorado, Universidade Federal do Pará, Belém, Brazil, 363p.

Journal Pre-proof

Fraga, L.M., Costa, J.B.S., 2004. Graben do Tacutu – Um exemplo da importância das Estruturas do Embasamento na evolução dos Riftes Mesozóicos no craton Amazônico. In: *42th Congresso Brasileiro de Geologia* (Araxá), CDROM.

Fraga, L.M.B., Almeida, M.E., Macambira, M.J.B., 1997. First lead-lead zircon ages of charnockitic rocks from Central Guiana Belt (CGB) in the state of Roraima, Brazil. In: *South-American Symposium on Isotope Geology*. Campos do Jordão, Brazil, Extended Abstracts, pp. 115-117.

Fraga L.M, Reis N.J., Dall'Agnol R., Armstrong R. 2008. Cauarane - Coeroene Belt - The Tectonic Southern Limit of the Preserved Rhyacian Crustal Domain in the Guyana Shield, Northern Amazonian Craton. *International Geological Congress*, Oslo, 6-14/8, 2008 – AMS-07. Crustal Evolution Of The Cratonic Nuclei of South America.

Fraga, L.M., Macambira, M.J.B., Dall'Agnol, R., Costa, J.B.S., 2009a. 1.94–1.93 Ga charnockitic magmatism from the central part of the Guyana Shield, Roraima, Brazil: Single zircon evaporation data and tectonic implications. *Journal of South American Earth Sciences* 27, 247-257.

Fraga, L.M., Dall'Agnol, R., Costa, J.B.S., Macambira, M.J.B., 2009b. The mesoproterozoic Mucajaí anorthosite – mangerite – rapakivi granite complex, Amazonian Craton, Brazil. *The Canadian Mineralogist* 47, 1469-1492.

Fraga L.M., Reis N.J., Dall'Agnol R. 2009c. Cauarane – Coeroeni Belt: The Main Tectonic Feature of the Central Guyana Shield, Northern Amazonian Craton. In: SBG-Núcleo Norte, Geological Amazonian Simposium, 11, Manaus, Amazonas State, *Expanded* Abstract, 4p.

Fraga L.M., Cordani U., Kroonenberg S., Roever de E., Nadeau S., Maurer V.C. 2017. U-Pb SHRIMP New Data On The High-Grade Supracrustal Rocks Of The Cauarane-Coeroeni Belt – Insights On The Tectonic Eo-Orosirian Evolution of the Guiana Shield. In: SBG/Núcleo Norte, Geological Amazonian Simposium, 15, Belém, Pará State, *Expanded Abstract*, 486-490.

Gaudette, H.E., Mendoza, V., Hurley, P.M., Fairbairn, H.W., 1978. Geology and age of the Parguaza rapakivi granite, Venezuela. *Geological Society of America Bulletin* 89, 1335-1340.

Gaudette, H.E., Olszewski, W.J., Santos, J.O.S. dos, 1996. Geochronology of Precambrian rocks from the northern part of Guiana Shield, state of Roraima, Brazil. *Journal of South American Earth Sciences* 9, 183–195.

Geraldes, M.C., Nogueira, C., Vargas-Mattos, G., Matos, R., Teixeira, W., Valencia, V., Ruiz, J., 2014. U-Pb detrital zircon ages from the Aguapeí Group (Brazil) : Implications for the geological evolution of the SW border of the Amazonian Craton. *Precambrian Research* 244, 306-316.

Gower, C.F., Ryan, A.B., Rivers, T., 1990, Mid-Proterozoic Laurentia-Baltica: An overview of its geological evolution and a summary of the contributions made by this volume, in Gower, C.F., Rivers, T., and Ryan, A.B., eds., Mid-Proterozoic Laurentia-Baltica. *Geological Association of Canada Special Paper* 38, 1–20.

Halls, H.C., Hamilton, M.A., Denyszyn, S.W., 2011. The Melville Bugt dyke swarm of Greenland: A connection to the 1.5–1.6 Ga Fennoscandian Rapakivi Granite Province? In: Srivastava, R.K. (Ed.), Dyke Swarms: Keys for Geodynamic Interpretation. Springer-Verlag, Berlin, pp. 509-535.

Hamilton, M. A., Buchan, K. L., 2010. U–Pb geochronology of the Western Channel Diabase, northwestern Laurentia: Implications for a large 1.59 Ga magmatic province, Laurentia's APWP and paleocontinental reconstructions of Laurentia, Baltica and Gawler craton of southern Austrália. *Precambrian Research* 183, 463–473.

Harlan, S.S., Geissman, J.W., 1998. Paleomagentism of the Middle Proterozoic Electra Lake Gabbro, Needle Mountains, southwestern Colorado. *Journal of Geophysical Research* 103, 15497–15507.

Harlan, S.S., Snee, L.W., Geissman, J.W., Brearley, A.J., 1994. Palaeomagnetism of the Middle Proterozoic Laramie anorthosite complex and Sherman Granite, South-ern Laramie Range, Wyoming and Colorado. *Journal of Geophysical Research* 99, 17997–18020.

Harlan, S.S., Geissman, J.W., Snee, L.W., 2008. Paleomagnetism of Proterozoic mafic dikes from the Tobacco Root Mountains, southwest Montana. *Precambrian Research* 163, 239–264.

Heinonen, A.P., Fraga, L.M., Rämö, O.T., Dall'Agnol, R., Mänttäri, I, Andersen, T., 2012. Petrogenesis of the igneous Mucajaí AMG complex, northern Amazonian craton — Geochemical, U–Pb geochronological, and Nd–Hf–O isotopic constraints. *Lithos* 151, 17–34.

Hoffman, P.F. 1991. Did the breakout of Laurentia turn Gondwanaland inside-out? *Science* 252, 1409-1412.

Irving, E., Donaldson, J.A., Park, J.K., 1972. Palaeomagnetism of the Western Channel diabase and associated rocks. Northwest Territories. *Canadian Journal of Earth Sciences* 9, 960-971.

Irving, E., Baker, J., Hamilton, M., Wynne, P.J., 2004. Early Proterozoic geomagnetic field in western Laurentia: implications for paleolatitudes, local rotations and stratigraphy. *Precambrian research* 129, 251-270.

Johansson, A., 2009, Baltica, Amazonia and the SAMBA connection—1000 million years of neighbourhood during the Proterozoic? *Precambrian Research* 175, 221–234.

Johansson, A., 2014. From Rodinia to Gondwana with the 'SAMBA' model – a distant view from Baltica towards Amazonia and beyond. *Precambrian Research* 244, 226-235.

Kirscher, U., Liu, Y., Li, Z.X., Mitchell, R.N., Pisarevsky, S.A., Denyszyn, S.W., Nordsvan, A., 2019. Paleomagnetism of the Hart Dolerite (Kimberley, Western Australia) – A two-stage assembly of the supercontinent Nuna? Precambrian Research (in press).

Kirschvink, J. L., 1980. The least-squares line and plane and the analysis of palaeomagnetic data. *Geophysics Journal Research of Astronomical Society* 62, 699-718.

Klein E.L., Almeida M.E., Rosa-Costa L.T. 2012. The 1.89-1.87 Ga Uatumã Silicic Large Igneous Province, northern South America. November 2012 LIP of the Month. http://www.largeigneousprovinces.org/12nov.

Llanos, M.P.I., Prezzi, C.B., 2013. The role of true polar Wander on the Jurassic paleoclimate. *International Journal of Earth Sciences (Geol. Rundsch)* 102, 745-759.

Lubnina, N.V., Mertanen, S., Söderlund, U., Bogdanova, S., Vasilieva, T.I., Frank-Kamenetsky, D., 2010. A new key pole for the East European Craton at 1452 Ma: palaeomagnetic and geochronological constraints from mafic rocks in the Lake Ladoga region (Russian Karelia). *Precambrian Research* 183, 442–462.

McFadden, P. L., McElhinny, M. W., 1995. Combining groups of paleomagnetic directions or poles. *Geophysical Research Letters* 22, 2191-2194.

Marzoli A., Renne P.R., Piccirillo E.M., Ernesto M., Bellieni G., De Min A., 1999. Extensive 200-million-year-old continental flood basalts of the Central Atlantic Magmatic Province. *Science* 284, 616-618.

Marzoli A., Bertrand H., Night K.B., Cirilli S., Buratti N., Vérati C., Nomade S., Renne P.R., Yoube N., Martini R., Allenbach K., Neuwerth R., Rapaille C., Zaninetti L., Bellieni G. 2004. Synchrony of the Central Atlantic magmatic province and the Triassic-Jurassic boundary climatic and biotic crisis. *Geological Society of America Bull*., 32 (11): 973–976.

Meert, J. G. 2002. Paleomagnetic Evidence for a Paleo-Mesoproterozoic Supercontinent Columbia. *Gondwana Research* 5, 207-215.

Meert, J. G. 2012. What's in a name? The Columbia (Paleopangaea/Nuna) supercontinent. *Gondwana Research* 21, 987-993.

Meert, J.G., Stuckey, W., 2002. Revisiting the paleomagnetism of the 1.476 Ga St. Francois Mountains igneous province. Missouri. *Tectonics* 21 (10.1029/2000TC001265).

Meert, J.G., Santosh, M., 2017. The Columbia supercontinent revisited. *Gondwana Research* 50, 67-83.

Mertanen, S., Pesonen, L.J., 1995. Palaeomagnetic and rock magnetic investigations of the Sipoo Sub-jotnian quartz porphyry and diabase dykes, southern Fennoscandia. *Physics of the Earth and Planetary Interiors* 88, 145-175.

Neuvonen, K.J., 1986. On the direction of remanent magnetization of the quartz porphyry dikes in SE Finland. *Bulletin of the Geological Society of Finland* 58, 195-201.

Nomade S., Knight K.B., Beutel E., Renne P.R., Verati C., Féraud G., Marzoli A., Youbi N., Bertrand H. 2007. Chronology of the Central Atlantic Magmatic Province: Implications for the Central Atlantic rifting processes and the Triassic–Jurassic biotic crisis. *Palaeogeography, Palaeoclimatology, Palaeoecology* 244: 326–344.

Onstott, T.C.; Hall, C.M. and York, D., 1989. ^{40}Ar/^{39}Ar thermochronometry of the Imataca Complex, Venezuela. *Precambrian Research* 42, 255-291.

Onstott, T.C., Hargraves, R.B., York, D., 1984. Dating of Precambrian diabase dikes of Venezuela using paleomagnetic and ^{40}Ar/^{39}Ar methods. *Anais II Symposium Amazônico*, Manaus, Brazil, DNPM 2, 513-518.Park, J.K., Inving, E., Donaldson, J.A., 1973. Paleomagnetism of the Precambrian Dubawnt Group. *Geological Society of American Bulletin* 103, 522–537.

Pehrsson, S.J., Eglington, B.M., Evans, D.A.D, Huston, D., Reddy, S.M., 2016. Metallogeny and its link to orogenic style during the Nuna supercontinent cycle. In: Li, Z. X., Evans, D. A. D., Murphy, J. B. (eds) Supercontinent Cycles Through Earth History. *Geological Society, London, Special Publications* 424, 83-94.

Pesonen, L.J., Neuvonen, K.J., 1981. Palaeomagnetism of the Baltic Shield – implications for Precambrian tectonics. In: Kroner, A. (Ed.), Precambrian Plate Tectonics. Elsevier, 623–648.

Pesonen, L.J., Mertanen, S., Veikkolainen, T., 2012. Paleo-Mesoproterozoic Supercontinents – A paleomagnetic view. *Geophysica* 47, 5-47.

Pesonen, L.J., Elming, S-A., Mertanen, S., Pisarevsky, S., D'Agrella-Filho, M.S., Meert, J. G., Schmidt, P.W. Abrahamsen, N., Bylund, G., 2003. Palaeomagnetic configuration of continents during the Proterozoic. *Tectonophysics* 375, 289-324.

Journal Pre-proof

Piper, 1992. Palaeomagnetism of the Almunge alkaline complex and Tuna dyke, Sweden: Mid-Proterozoic palaeopoles from the Fennoscandian Shield. *Geologiska Föreningens i Stockholm Förhandlingar* 114, 291-297.

Piper, J.D.A., Smith, R.L., 1980. Palaeomagnetism of the Jotnian lavas and sediments and post-Jotnian dolerites of central Scandinavia. *Geologiska Föreningens i Stockholm Förhandlingar* 102, 67-81.

Pisarevsky, S. A., Bylund, G. 2010. Paleomagnetism of 1780–1770 Ma mafic and composite intrusions of Småland (Sweden): Implications for the Mesoproterozoic Supercontinent. *American Journal of Science* 310, 1168–1186.

Pisarevsky, S.A., Sokolov, S.J., 2001. The magnetostratigraphy and a 1780 Ma palaeomagnetic pole from the red sandstones of the Vazhinka River section, Karelia, Russia. *Geophysical Journal Interiors* 146, 531-538.

Pisarevsky, S.A., Elming, S.Å., Pesonen, L.J., Li, Z.X. 2014. Mesoproterozoic paleogeography: Supercontinent and beyond. *Precambrian Research* 244, 207–225.

Pullaiah, G., Irving, E., Buchan, K.L., Dunlop, D.J., 1975. Magnetization changes caused by burial and uplift. *Earth and Planetary Science Letters* 28, 133-143.

Rämö, O.T., Haapala, L., 2005. Rapakivi granites. In: Lehtinen, M., Nurmi, P.A., Rämö, O.T., (Eds.) Precambrian Geology of Finland – Key to the Evolution of the Fennoscandian Shield. Elsevier, Asterdam, pp. 533-562.

Rämö, N.J., McLemore, V.T., Hamilton, M.A., Kosunen, P.J., Heizler, M., Haapala, L., 2003. Intermittent 1630-1220 Ma magmatism in central Mazatzal Province: new geochronologic piercing points and some tectonic implications. *Geology* 31, 335-338.

Reis, N.J., Fraga, L.M.B., Faria, M.S.G. de, Almeida, M.E., 2003. Geologia do Estado de Roraima, Brasil. In: *Geologie de La France*, vols. 2-4, pp. 121-134.

Reis N.J., Faria M.S.G., Almeida M.E., Oliveira M.A., 2004. Folhas NA.20-Boa Vista e NB.20-Roraima. *In*: C. Schobbenhaus, J.H. Gonçalves, J.O.S. Santos, M.B. Abram, R. Leão Neto, G.M.M. Matos, R.M. Vidotti, M.A.B. Ramos, J.D.A. de Jesus (eds.). *Carta Geológica do Brasil ao Milionésimo*, Sistema de Informações Geográficas - SIG. Programa Geologia do Brasil. CPRM, Brasília. Edição 2004. CD-ROM.

Reis N.J., Szatmari P., Wanderlei Filho J.R., York D., Evensen N.M., Smith P.E., 2006. Dois Eventos de Magmatismo Máfico Mesozóico na Fronteira Brasil – Guiana, Escudo das Guianas: Enfoque à Região do Rifte Tacutu – North Savannas. *In*: M.G.Silva, W.J.S. Franca-Rocha (org.), Coletânea de Trabalhos Completos, SBG, Congresso Brasileiro de Geologia, 43, Aracaju, S14_02, 2006, CD-ROM.

Reis, N.J., Teixeira, W., Hamilton, M.A., Bispo-Santos, F., Almeida, M.E., D'Agrella-Filho, M.S. 2013. The Avanavero mafic magmatism, a late Paleoproterozoic LIP in the Guiana Shield, Amazonian Craton: U-Pb TIMS baddeleyite, geochemical and paleomagnetic evidence. *Lithos* 174, 175-195.

Rizzotto, G.J., Scandolara, J.E., Quadros, M.L.E.S., 1996. Aspectos da Associação Mangerito-Charnockito-granito (MCG) da porção oriental do estado de Rondônia. In: *39th Congresso Brasileiro de Geologia*, Salvador. Anais, SBG, 7 v.1, p.35-37.

Roberts, A.P., Heslop, D., Zhao, X., Pike, C.R., 2014. Understanding fine magnetic particle systems through use of first-order reversal curve diagrams. *Reviews of* Geophysics 52, 557-602.

Roest, W.R., Srivastava, S.P., 1989. Sea-floor spreading in the Labrador Sea: a new reconstruction. Geology 17(11), 1000-1003

Journal Pre-proof

Rogers, J.J.W., Santosh, M. 2002. Configuration of Columbia, a Mesoproterozoic Supercontinent. *Gondwana Research* 5, 5-22.
Rogers, J.J.W., Santosh, M. 2009. Tectonics and surface effects of the supercontinent Columbia. *Gondwana Research* 15, 373-380.
Salminen, J., Pesonen, L.J. 2007. Paleomagnetic and rock magnetic study of the Mesoproterozoic sill, Valaam island, Russian Karelia. *Precambrian Research* 159, 212–230.
Salminen, J., Pesonen, L.J., Mertanen, S., Vuollo, J., Airo, M.-L., 2009. Palaeomagnetism of the Salla Diabase Dyke, northeastern Finland, and its implication for the Baltica-Laurentia entity during the Mesozoic., In: Reddy, S.M., Mazunder, R., Evans, D.A.D., Collins, A.S. (eds.) Palaeoproterozoic Supercontinents and Global Evolution. *Geological Society, London, Special Publications* 323, 199-217.
Salminen, J., Mertanen, S., Evans, D.A.D., Wang, Z., 2014. Paleomagnetic and geochemical studies of the Mesoproterozoic Satakunta dyke swarms, Finland, with implications for a Northern Europe – North America (NENA) connection within Nuna supercontinent. *Precambrian Research* 244, 170-191.
Salminen, J.M., Klein, R., Mertanen, S., Pesonen, L.J., Fröjdö, S., Mänttäri, I., Eklund, O, 2016a. Palaeomagnetism and U-Pb geochronology of ca. 1570 Ma intrusives from Åland archipelago, SW Finland implications for Nuna. In: Li, Z. X, Evans, D.A.D. and Murphy, J.B. (eds.): Supercontinent Cycles Through Earth History. *Geological Society, London Special Publications* 424, 95-118.
Salminen, J.M., Evans, D.A.D., Trindade, R.I.F., Oliveira, E.P., Piispa, E.J., Smirnov, A.V., 2016b. Paleogeography of the Congo/São Francisco craton at 1.5 Ga: expanding the core of Nuna supercontinent. *Precambrian Research* 286, 195-212.
Salminen, J.M, Klein, R., Veikkolainen, T., Mertanen, S., Mänttäri, I., 2017. Mesoproterozoic geomagnetic reversal asymmetry in light of new paleomagnetic and geochronological data for the Häme dyke swarm, Finland: Implications for the Nunasupercontinent. *Precambrian Research* 288, 1-22.
Santos, J.O.S.; Reis., N.J.; Hartman, L.A; McNaugthon, N.J.; Fletcher, I.R. 1999. Associação Anortosito-Charnockito-Granito Rapakivi no Calimiano do Norte do Cráton Amazônico, Estado de Roraima: Evidências Obtidas por Geocronologia U-Pb (SHRIMP) em zircão e baddeleyíta. In: Simpósio de Geologia da Amazônia, 6, Manaus. Anais... Manaus: SBG, Núcleo Norte, p. 503-506.
Santos, J. O. S., Hartmann, L. A., Gaudette, H. E., Groves, D. I., McNaugthon, N.J., Fletcher, I. R. 2000. A new understanding of the Provinces of Amazon Craton based on integration of field mapping and U-Pb and Sm-Nd geochronology. *Gondwana Research* 3, 453-488.
Santos J.O.S., Hartmann L.A., Faria M.S.G. de, Riker S.R.L., Souza M.M. de, Almeida M.E., McNaughton N.J. 2006. A Compartimentação do Cráton Amazonas em Províncias: Avanços ocorridos no período 2000-2006. *In*: SBG-Núcleo Norte, Geological Amazonian Simposium, 9, Belém, Pará State, *Expanded Abstract*, 4p.
Santos, J.O.S., Pinto, V., McNaughton, N.J., Silva, L.C., 2011. O magmatismo Serra Grande em Roraima: Formação co-genética de granito rapakivi e charnockito em ca. 1430 Ma. In: *12º Simpósio de Geologia da Amazônia*, Boa Vista, Roraima, 4p.
Scandolara, J.E., Fuck, R.A., Dall'Agnol, R., Dantas, E.L., 2013. Geochemistry and origin of the early Mesoproterozoic mangerite–charnockite–rapakivi granite association of the Serra da Providência suite and associated gabbros, central–eastern Rondônia, SW Amazonian Craton, Brazil. *Journal of South American Earth Sciences* 45, 166-193.

Schobbenhaus, C., Goncalves, J. H., Santos, J. O. S., Abram, M.B., Leão Neto, R., Matos, G. M. M., Vidotti, R. M., Ramos, M. A. B., Jesus, J. D. A. 2004. *Carta Geológica do Brasil ao Milionésimo*. Sistema de Informações Geográficas. Folhas Boa Vista (NA-20) e Roraima (NB-20). Escala 1:1,000,000. CPRM.

Shcherbakova, V.V., Pavlov, V.E., Shcherbakov, V.P., Neronov, I., Zemtsov, V.A., 2006. Palaeomagnetic studies and estimetion of geomagnetic palaeointensity at the Early/ Middle Riphean boundary in rocks of the Salmi formation (north Ladoga area). *Izvestiya Physics Solid Earth* 42, 233-243.

Shumlyanskyy, L., Howkesworth, C., Billström, K., Bogdanova, S., Mytrokhym, O., Romer, R., Dhuime, B., Claesson, S., Ernst, R., Whitehouse, M., Bilan, O., 2017. The origin of the Palaeoproterozoic AMCG complexes in the Ukrainian shield: New U-Pb ages and Hf isotopes in zircon. *Precambrian Research* 292, 216-239.

Silver, P.G., Behn, D., 2008. Intermittent plate tectonics. *Science* 319, 85-88.

Smirnov, A.V., 2017. Intensity of Geomagnetic Field in the Precambrian and Evolution of the Earth's Deep Interior. *Izvestiya, Physics of the Solid Earth* 53, 760–768.

Smirnov, A.V., Tarduno, J.A., Evans, D.A.D., 2011. Evolving core conditions ca. 2 billion years ago detected by paleosecular variation. *Physics of the Earth Planetary Interiors* 187, 225–231.

Söderlund, U., Isachsen, C.E., Bylund, G., Heaman, L.M., Patchett, P.J., Vervoort, J.D., Andersson, U.B., 2005. U-Pb baddeleyite ages and Hf, Nd isotope chemistry constraining repeated mafic magmatism in the Fennoscandian Shield from 1.6 to 0.9 Ga. *Contributions to Mineralogy and Petrology* 150, 174-194.

Tassinari, C.C.G., Macambira, M.J.B. 1999. Geochronological provinces of the Amazonian Craton. *Episodes* 22, 174–182.

Tassinari C.C.G., Macambira M.J.B. 2004. A evolução tectônica do Cráton Amazônico. In: Mantesso-Neto V., Bartorelli A., Dal Ré Carneiro C., Brito Neves B.B. (eds.) *Geologia do Continente Sul-Americano: Evolução da obra de Fernando Flávio Marques de Almeida*. São Paulo, Ed. Beca, p. 471-485.

Teixeira, W., Ernst, R.E., Hamilton, M.A., Lima, G., Ruiz, A.S., Geraldes, M.C., 2015. Widespread 1.4 Ga intraplate magmatism and tectonics in a growing Amazonia. *GFF* http://dx.doi.org/10.1080/11035897.2015.1042033

Teixeira, W., Geraldes, M.C., D'Agrella-Filho, M.S., Santos, J.O.S., Barros, M.A.S., Ruiz, A.S., Costa, P.C.C., 2011. Mesoproterozoic juvenile mafic-ultramafic magmatism in the SW Amazonian Craton (Rio Negro-Juruena province): SHRIMP U-Pb geochronology and Nd-Sr constraints of the Figueira Branca Suite. *Journal of South American Earth Sciences* 32, 309-323.

Teixeira W., Reis N.J., Bettencourt J.S., Klein E.L., Oliveira D.C. 2019. Intraplate Proterozoic Magmatism in the Amazonian Craton reviewed: geochronology, crustal tectonics and global barcode matches. In: R. K. Srivastava et al. (eds.), *Dyke Swarms of the World: A Modern Perspective*, Springer Geology, https://doi.org/10.1007/978-981-13-1666-1_4.

Tohver, E., van der Pluijm, B.A., Van der Voo, R., Rizzotto, G., Scandolara, J.E., 2002. Paleogeography of the Amazon craton at 1.2 Ga: early Grenvillian collision with the Llano segment of Laurentia. *Earth and Planetary Science Letters* 199, 185-200.

Torsvik, T.H., Van der Voo, R., Preeden, U., Mac Niocaill, C., Steinberger, B., Doubrovine, P.V., Van Hinsbergen, D.J.J., Domier, M., Gaina, C., Tohver, E., Meert,

Journal Pre-proof

J.G., McCausland, P.J.A., Cocks, L.R.M., 2012. Phanerozoic polar wander, palaeogeography and dynamics. *Earth-Science Reviews* 114, 325–368.

Van der Voo, R. 1990. The reliability of paleomagnetic data. *Tectonophysics* 184, 1-9.

Valdespino, O.E.M., Costanzo-Alvarez, V., 1997. Paleomagnetic and rock magnetic evidence for inverse zoning in the Parguaza batholith (southwestern Venezuela) and its implications about tectonics of the Guyana shield. *Precambrian Research* 85, 1-25.

Veikkolainen, T., Pesonen, L.J., 2014. Palaeosecular variation, field reversals and the stability of the geodynamo in the Precambrian. *Geophysical Journal International* 199, 1515–1526

Veikkolainen, T., L.J. Pesonen, A. Heinonen, L.M. Fraga, O.T. Rämö and R. Dall'Agnol, 2011. Paleomagnetism of the Mucajai rapakivi anorthosite complex, Roraima batholite, Amazonia. In: Kaikkonen, P., Kaila, K., Kozlovskaya, E., Moisio, K. and Pirttijärvi, M., 2011 (Eds.). XXV Geofysiikan päivät, Oulu, Finland, May 11–12, 2011, *Geophysical Society of Finland*, 121–124.

Vigneresse, J.L., 2005. The specific case of the Mid-Proterozoic rapakivi granites and associated suite within the context of the Columbia Supercontinent. *Precambrian Research* 137, 1-34.

Xu, H., Yang, Z., Peng, P., Meert, J.G., Zhu, R., 2014. Paleo-position of the North China craton within the Supercontinent Columbia: Constraints from new paleomagnetic results. *Precambrian Research* 255, 276-293.

Zhang, S., Li, Z.-X., Evans, D.A.D., Wu, H., Li, H., Dong, J., 2012. Pre-Rodinia supercontinent NUNA shaping up: A global synthesis with new paleomagnetic results from North China. *Earth Planetary Science Letters* 353-354, 145-155.

Zhao, G., Cawood, P.A., Wilde, S.A., and Sun, M., 2002, Review of global 2.1–1.8 Ga orogens: Implications for a pre-Rodinia supercontinent: *Earth-Science Reviews* 59, 125–162.

Zijderveld, J. D. A., 1967. A. C. Demagnetization of Rocks: Analysis of Results. In: Collinson, D. W.; Creer, K. M. Runcorn, S. K. (eds) Methods in Paleomagnetism, pg. 254-286.

Journal Pre-proof

FIGURE CAPTIONS

FIGURE 1: A – Amazonian Craton and their geochronological provinces (Cordani and Teixeira, 2007): CA – Central Amazon (>2,6 Ga), MI – Maroni-Itacaiunas (2,25-2,05 Ga), VT – Ventuari-Tapajós (2,00-1,80 Ga), RNJ – Rio Negro-Juruena (1,78-1,55 Ga), RO – Rondonian-San Ignacio (1,50-1,30 Ga), SS – Sunsas-Aguapeí (1,25-1,00 Ga).ra – Rio Apa Craton, np – Neoproterozoic Provinces, ab – Andean belt, pc – Phanerozoic cover; B – Simplified Geological Map of the Guiana Shield (after Fraga et al., 2017): Orosirian/Calimian - IMSCD – Imeri-San Carlos Domain (1,81-1,79 Ga), UIB – Uatumã Igneous Belt (1,90-1,87 Ga), OIB – Orocaima Igneous Belt (1,98-1,95 Ga), PSB –

Journal Pre-proof

Pakaraima Sedimentary Block (1,95-1,87 Ga), RUIB – Rio Urubu Igneous Belt (1,95-1,93 Ga), AMG Complex (1,56-1,47 Ga), PA-KW – Parima-Kwitaro Supracrustals (1,96-1,94 Ga), CCB – Cauarane-Coeroeni Belt (~ 2,0 Ga), T-A gneisses/metagranitoids (2,04-2,02 Ga). Rhyacian – Bk – Bakhuis (2,06 Ga), Granite-Greenstone Belts (2,21-2,07 Ga), Archean (reworked) – IB – Imataca Block and AB – Amapá Block; C – Geological map showing the AMG Complex and the Serra Grande Suite (after Fraga, 2002) and sampling sites (circles, this paper).

FIGURE 2: Normalized magnetization intensities (M/Mo) versus (a) alternating magnetic field (H) and (b) temperature (T) for samples from different sites. A – Anorthosite; G – Granite; M – Mangerite.

FIGURE 3: (a-d) Examples of hysteresis curves (magnetic moment (J) versus magnetic field (H)), showing narrow waist characteristic of titanomagnetite/magnetite; (e) Day's diagram (Day et al., 1977) after Dunlop (2002) ploting Mrs/Ms versus Hcr/Hc ratios. Most samples fall in the Pseudo-single domain (PSD field), or along the SD (Single domain) plus MD (Multidomain) mixing curves as proposed by Dunlop (2002). Percentages of MD grains in the mixture are also shown.

FIGURE 4: FORC diagrams (Hb – reversal field) for selected samples. A – Anorthosite; G – Granite; M – Mangerite.

FIGURE 5: Typical thermomagnetic curves showing variation in magnetic susceptibility K(SI) versus low and high temperature. Curves were corrected from furnace effects. Heating in red and cooling in blue. A – Anorthosite; G – Granite; M – Mangerite.

FIGURE 6: Examples of IRM acquisition curves (normalized intensities versus magnetic field). A – Anorthosite; G – Granite; M – Mangerite.

FIGURE 7: Examples of magnetic component disclosed for six samples from different sites of the Mucajaí rocks after AF and thermal demagnetizations. The figure shows stereographic projections (solid (open) symbols represent positive (negative) inclinations), normalized magnetization intensity curves (M/Mo versus alternating field (H) or temperature) and orthogonal projections (solid (open) symbols represent horizontal (vertical) projections) for each sample. A – Anorthosite; G – Granite; M – Mangerite.

FIGURE 8: Site mean directions: component A with normal and reverse directions in (a), and after inversion of one of the polarities in (b); Component B with normal and

Journal Pre-proof

reverse directions in (c), and after inversion of one of the polarities in (d). Full (empty) circles represent downward (upward) inclinations. Plus signal inside yellow circle represents the mean of site mean directions with its respective confidence circle (α95). The red, blue and green circles represent the lithologies of the sites, respectively, granites, mangerites and anorthosites. Dark and pink circles represent the sites included by Veikkolainen et al. (2011) and Serra Grande Suite, respectively. PDF – Present Dipolar Geomagnetic field; PGF – Present Geomagnetic Field.

FIGURE 9: Examples of magnetic component disclosed for samples from two sites of the Serra Grande Suite rocks after AF demagnetization. The figure shows stereographic projections (solid (open) symbols represent positive (negative) inclinations), normalized magnetization intensity curves (M/Mo versus alternating field (H) or temperature) and orthogonal projections (solid (open) symbols represent horizontal (vertical) projections) for each sample. G – Granite; M – Mangerite.

FIGURE 10: (a) Comparation of MC/SG-B pole (component B) with an apparent polar wander path traced for South America between 215 Ma and 160 Ma (modified after Llanos and Prezzi, 2013), whose time includes the ca. 200 Ma CAMP event. (b) Comparison of the Mucajai Complex MC-A (component A) paleomagnetic pole with the 1200 Ma (Nova Floresta) NFF pole (Tohver et al., 2002) and the 1540 Ma Parguaza pole (Valdespino and Costanzo-Alvarez, 1997). Stands out that the (ca. 1200 Ma) K'Mudku event in Amazonian Craton affected the southern portion Mucajaí Complex. (see text for details).

FIGURE 11: (a) Paleogeographic reconstruction of Laurentia, Baltica and proto-Amazonia (core of Columbia) at 1530 Ma (Baltica and Amazonia as in a SAMBA-like connection of Johansson, 2009). Euler rotation poles used: Laurentia (39.6°N, 290.0°E, -115.0°), Baltica (42.98°N, 243.9°E, -96.75°) and Amazonian Craton (9.28°N, 75.8°E: 32.5°). (b) Rotated 1590 Ma - 1525 Ma paleomagnetic poles (Table 2) from Laurentia, Baltica and Amazonia. These poles are grouped indicating the compatibility of the proposed paleogeographic model in (a). *Laurentia (LA) in blue; Baltica (BA) in red; and Amazonian Craton (CA) in yellow. Archaean cratonic areas and Paleoproterozoic belts (dark gray): Laurentia (S – Slave; C – Churchill; SU – Superior; N – Nain, NQ – New Quebec; T – Tornget; W – Wopmay; P – Penokean; K – Kefilidian; NA – Nagssugtoqidian; FR – Foxe-Rinklan), Baltica (KO – Kola; KA – Karelia, LK – Lapland-Kola; SD – Svecofennian Domain; G – Gothian Province), Amazonian Craton (CA – Central Amazonian, MI – Maroni-Itacaiunas; VT – Ventuari-Tapajos; RNJ – Rio Negro-Juruena).*

Journal Pre-proof

Journal Pre-proof

FIGURE 12: Paleomagnetic poles in the interval between 1780 Ma and 1400 Ma (Table 2) for Laurentia (LA), Baltica (BA) and Amazonian Craton (CA). These poles were rotated using the Euler rotation poles (Table 2) used in the configuration proposed for the core of Columbia (Fig. 11). An apparent polar wander path is traced showing the possibility of a rupture of Columbia at ca. 1440-1420 Ma (see text for details). Laurentia (LA), Baltica (BA) and Amazonia (CA) poles in blue, red and yellow, respectively.

TABLE CAPTIONS

TABLE 1: Paleomagnetic results of the Mucajai AMG Complex and Serra Grande Suite.

Footnotes: Slat, Slong – site latitude and longitude (geographic coordinates); G – Rapakivi Granite, M – Mangerite, A – Anorthosite; N / n - *number of specimens used in mean directions / number of analyzed specimens; Dec* – Declination; Inc – Inclination; α_{95}/A_{95} *and k/K - Fisher's statistical parameters for mean directions / mean virtual geomagnetic poles, respectively*; VGP – Virtual Geomagnetic Pole; Plat – pole latitude; Plong – pole longitude; Ref.: 1 - This work; 2 - Veikkolainen et al. (2011). MC-A and MC/SG-B poles were calculated by the mean of their respective VGPs.

TABLE 2: Selected paleomagnetic poles between 1780 Ma and 1430 Ma for Amazonian Craton, Baltica and Laurentia.

Footnotes: *Plat (Paleolatitude); Plong (Paleolongitude); Euler poles (used for each cratonic block);* A_{95} *(confidence circle - Fisher's statistic parameters); Rlat (rotated latitude); Rlong (rotated longitude); Q (Quality factor, Van der Voo, 1990). * - The Melville Bugt pole from Greenland was first rotated to North America using the Euler pole: 67.5°N, 241.5°E, -13.8° (Roest and Srivastava, 1989). Ref.: 1-Bispo-Santos et al. (2014a); 2- Onstott et al. (1984); 3- Valdespino and Costanzo-Alvarez (1997); 4- This work; 5- D'Agrella-Filho et al. (2016a); 6-Geraldes et al. (2014); 7-Teixeira et al. (2015a); 8- Bispo-Santos et al. (2012); 9- D'Agrella-Filho et al. (2012); 10-Teixeira et al. (2011); 11-Fedotova et al. (1999); 12-Pisarevsky and Sokolov (2001); 13-Elming et al. (2009); 14-Pisarevsky and Bylund (2010); 15- Elming et al. (2018, in press); 16-Salminen et al. (2017); 17- Neuvonen (1986); 18- Mertanen and Pesonen (1995); 19-Salminen et al. (2015); 20-Salminen et al. (2014); 21-Piper and Smith (1980); 22- Piper (1992); 23- Shcherbakova et al. (2006); 24-Lubnina et al. (2010); 25-Salminen and Pesonen (2007); 26- Söderlund et al. (2005); 27- Park et al. (1973); 28- Irving et al. (2004); 29- Halls et al.*

Journal Pre-proof

(2011); 30- Irving et al. (1972); 31-Hamilton and Buchan (2010); 32-Meert and Stuckey (2002); 33-Emslie et al. (1976); 34-Harlan et al. (2008); 35- Elston et al. (2002); 36- Irving et al. (1977); 37-Elming and Pesonen (2010); 38- Harlan et al. (1994); 39-Harlan and Geissman (1998); 40- Elston and Bressler (1980).

Journal Pre-proof

Journal Pre-proof

Sites	Slat(°N)/Slon(°W)	Samples	Rock Type	N/n	Site Mean Directions				VGP		Ref.
					Dec(°)	*Inc(°)*	*α_{95}(°)/A_{95}(°)*	*k/K*	*Plat(°N)*	*Plong(°E)*	
2	2°26'16.1"/61°14'43.3"	FRM9	G	7/18	318.8	-35.3	6.0	101.7	-44.2	359.0	1
5	2°22'34.1"/61°14'20.4"	FRM12	G	12/21	169.1	41.2	9.2	23.0	-62.3	320.8	1
9	2°14'36.0"/61°31'44.5"	FRM16	M	16/20	283.4	-30.7	4.9	58.3	-12.2	11.6	1
10	2°15'17.2"/61°31'35.9"	FRM17	M	18/23	146.0	4.7	7.2	23.9	-55.7	21.9	1
11	2°15'48.9"/61°30'29.3"	FRM18	A	21/21	143.5	32.6	6.4	25.4	-49.0	358.7	1
12	2°15'49.6"/61°30'29.8"	FRM19	M	17/22	135.7	38.3	5.7	40.0	-40.7	358.0	1
13	2°13'33.3"/61°26'19.8"	FRM20	A	11/17	130.5	66.3	11.0	18.0	-23.7	332.2	1
14	2°12'11.3"/61°25'43.3"	FRM21	M	13/15	89.1	21.2	9.7	19.3	1.2	18.1	1
15	2°16'58.4"/61°22'0.0"	FRM22	G	15/21	140.1	60.0	6.5	36.0	-33.8	334.7	1
16	2°16'5.7"/61°21'46.1"	FRM23	M	9/24	132.6	16.0	7.1	53.8	-41.7	16.2	1
17	2°12'11.3"/61°24'34.8"	FRM24	G	11/20	174.7	20.8	9.3	25.2	-76.2	321.4	1
19	2°33'39.1'/61°21'48.6"	FRM26	G	10/21	133.8	39.8	11.5	18.6	-38.7	357.6	1
23*	-	R01	A	7	119.4	41.8	39.7	-	-25.7	1.0	2
24*	-	R02	G	3	138.4	26.7	44.2	-	-45.7	6.3	2
25*	-	R03	G	7	93.2	21.5	7.4	-	-2.8	17.7	2
		Mean		12	136.5	36.1	14.8	9.6			1
		Mean		15	132.2	35.4	12.7	10.0			1,2
		Pole		MC			14.4	10.1	-41.5	357.3	
		Pole		**MC-A**			**12.6**	**10.2**	**-38.2**	**0.1**	**1,2**
1	2°41'46.1"/61°10'19.3"	FRM8	G	19/27	227.5	33.8	6.6	27.2	-39.0	234.9	1
3	2°24'22.2"/61°14'44.4"	FRM10*	G	0/8	-	-	-	-	-	-	1
4	2°23'27.7"/61°14'43.3"	FRM11	G	13/20	226.1	7.1	10.1	17.9	-43.6	215.9	1
6	2°15'39.4"/61°20'28.9"	FRM13	G	10/20	245.1	-4.6	8.1	36.0	-24.9	207.4	1
7	2°15'41.6"/61°20'31.6"	FRM14	G	14/25	28.0	25.4	8.0	25.8	-60.1	185.2	1
8	2°14'36.6"/61°31'46.0"	FRM15	M	15/22	49.7	24.4	8.7	20.3	-39.7	194.0	1
18	2°14'01.1"/61°23'37.2"	FRM25*	G	13/27	283.4	27.5	15.8	7.8	-13.4	43.5	1
20	2°33'44.5'/61°21'19.3"	FRM27	G	14/17	247.1	-36.2	6.7	35.8	-22.1	188.1	1
21	2°33'27.8"/61°22'40.9"	FRM28*	G	0/15	-	-	-	-	-	-	
22	2°32'47.4"/61°30'03.5"	FRM29	G	9/16	228.5	21.1	6.0	74.5	-40.1	225.1	1
26	2°32'14.0"/60°47'51.2"	FRM2	M	4/10	53.0	-23.2	9.3	97.6	-35.5	226.4	1
27	2°34'32.6"/60°43'10.4"	FRM4	M	7/7	48.7	-27.6	8.6	49.9	-39.0	230.7	1
28	2°31'45.5"/60°48'10.8"	FRM5	G	9/16	44.7	24.8	10.1	26.7	-44.4	193.7	1
29	2°32'31.6"/60°48'06.4"	FRM6	G	16/16	22.2	-25.5	6.9	29.2	-63.1	245.6	1
		Mean		11	47.3	-2.7	17.5/	7.8/			1
		Pole		MC/SG-B			11.0	18.0	-42.6	212.7	1

Geologic Unit	Code	Plat (°N)	Plong (°E)	A95 (°)	Euler Pole	Rlat (N°)	Rlong (E°)	Age (Ma)	Q	Ref.
Amazonian Craton					*9.28°N;75.8°E(32.5°)*					
Avanavero Sills	AC1	48.4	207.9	9.6		62.11	258.21	1788.5±2.5	6	1
La Escalera/Aro/Guyana comp. I	AC2	59.0	222.0	7.0		60.20	286.0	1640 (Rb-Sr)	4	2
Parguaza*	AC3	54.4	173.7	9.6		83.14	232.02	1545±20	3	3
Mucajai Complex (Comp. A)	AC4	38.2	180.1	12.6		67.28	205.04	1530	6	4
Rio Branco Sedimentary Rocks	AC5	-45.5	270.0	6.5		45.44	61.41	1440	4	5,6
Salto do Céu Sills	AC6	-56.0	278.5	7.9		56.09	53.37	1439±4	5	5,7
Nova Guarita Dykes	AC7	-47.9	245.9	7.0		35.74	43.52	1418.5±3.5	6	8
Indiavai Dykes	AC8	-57.0	249.7	8.6		43.91	37.49	1416±7	4	9,10
Baltica					*42.98°N;243.9°E(-96.75°)*					
Ropruchey Sill		40.5	229.8	8.1				1770±12		11
Shosksha Formation		42.0	221.0	7.0				1790-1770		12
Hoting Gabbro		43.0	233.3	12.1				1786±10		13
Småland Intrusions		45.7	182.7	8.0				1784-1769		14
Mean	BA1	43.9	215.9	12.2		61.53	257.59	~1780		4
Turinge Gabbro-Diabase	BA2	51.6	220.2	4.8		54.4	265.5	1700		15
Häme DB dykes	BA3	23.6	209.8	14.7		73.15	209.80	1642±2	5	16
SE-Quartz porphire dykes	BA4	30.2	175.4	9.4		74.4	358.4	1617+2, 1639+9, 1638+53	4	17
Sipoo porphyre	BA5	26.4	180.6	9.4		80.0	8.7	1633 ± 10	3	18
Åland Intrusives		23.7	191.4	2.8				1575±3	6	19
Satakunta Dykes		29.3	188.1	6.6				1565	6	20
Dala Sandstones		32.1	184.5	20.8				1540	4	21
Mean	BA6	28.4	188.1	8.0		84.44	327.87	~1550		4
Tuna Dykes		21.0	180.0	7.0				1461-1462	3	22
Salmi Formation		6.0	200.0	11.0				1460	6	23
Lake Ladoka mafic rocks		15.0	177.0	5.5				1452±12	6	24
Valaam sills		14.0	166.0	2.4				$1458^{+4}/_{-3}$	5	25
Bunkris-Glysjön-Öje Dykes		28.3	179.8	13.2				1469±9	4	26
Mean	BA7	17.3	180.7	13.8		78.12	57.00	~1460		4
Oskarhamn-Alsterbo dolerites	BA8	6.8	173.2	14.1		65.70	67.52	1430	3	27
Laurentia					*38.4°N;280.4°E(-117.4°)*					
Dubawnt Group	LA1	7.0	277.0	8.0		49.27	238.65	1785±4	5	28
Cleaver dykes	LA2	19.4	276.7	6.1		48.22	257.44	1740 +5/−4	5	29
Melville Bugt dyke swarm	LA3	5.0	274.0	9.0		50.18	235.32	1622±3,1635±3	5	30
Western Channel Dykes	LA4	9.0	245.0	7.0		80.57	254.40	1592±3,1590±4	5	31,32
St. Francois mountains		-13.2	219.0	6.1				1476±16	6	33

Journal Pre-proof

Journal Pre-proof

Michikamau intrusion		-1.5	217.5	4.7			1460±5	6	34
Tabacco Root Dykes		9.0	216.0	10.0			1448±49	6	35
Spokane Formation		-24.8	215.5	4.7			1457	6	36
Harp Lake Compl.		1.6	206.3	4.0			1450±5	3	37
Mean	LA5	-5.7	214.8	13.5	65.84	83.17	~1460		4
Mean rocky mountain		-11.9	217.4	9.7			1430±15	5	37
Purcell lava		-23.6	215.6	4.8			1443±7	6	38
Laramie anorthosite		-6.7	215.0	3.5			1429±9	4	39
Electra Lake gabbro		-21.1	221.1	3.4			1433±2	4	40
Belt Supergroup		-18.9	207.2	5.6			1400-1470	4	41
Mean	LA6	-16.5	215.3	8.0	59.63	102.67	~1430		4
McNamara Formation	LA7	-13.5	208.3	6.7	56.32	90.16	1401±6	7	38

*Footnotes: Plat (Paleolatitude); Plong (Paleolongitude); Euler poles (used for each cratonic block); A_{95} (confidence circle - Fisher's statistic parameters); Rlat (rotated latitude); Rlong (rotated longitude); Q (Quality factor, Van der Voo, 1990). * - The Parguaza pole was recalculated using the selected sites CSP-3-6, PI4-1A, PI4-1BT, PI4-2BT, PI4-4T and PI2-8T from Table 1 (component G1) of Valdespino and Costanzo-Alvarez (1997). Ref.: 1-Bispo-Santos et al. (2014a); 2-Onstott et al. (1984); 3- Valdespino and Costanzo-Alvarez (1997); 4- This work; 5- D'Agrella-Filho et al. (2016a); 6-Geraldes et al. (2014); 7-Teixeira et al. (2015a); 8- Bispo-Santos et al. (2012); 9- D'Agrella-Filho et al. (2012); 10-Teixeira et al. (2011); 11-Fedotova et al. (1999); 12-Pisarevsky and Sokolov (2001); 13-Elming et al. (2009); 14-Pisarevsky and Bylund (2010); 15- Elming et al. (2018, in press); 16-Salminen et al. (2017); 17- Neuvonen (1987); 18- Mertanen and Pesonen (1995); 19-Salminen et al. (2015); 20-Salminen et al. (2014); 21-Piper and Smith (1980); 22- Piper (1992); 23-Shcherbakova et al. (2006); 24-Lubnina et al. (2010); 25-Salminen and Pesonen (2007); 26- Söderlund et al. (2005); 27- Pisarevsky and Bylund (2010); 28-Park et al. (1973); 29- Irving et al. (2004); 31- Irving et al. (1972); 32-Hamilton and Buchan (2010); 33-Meert and Stuckey (2002); 34-Emslie et al. (1976); 35-Harlan et al. (2008); 36- Elston et al. (2002); 37-Elming and Pesonen (2010); 38- Halls et al. (2011); 39-Harlan et al. (1994); 40-Harlan and Geissman (1998); 41- Elston and Bressler (1980).*

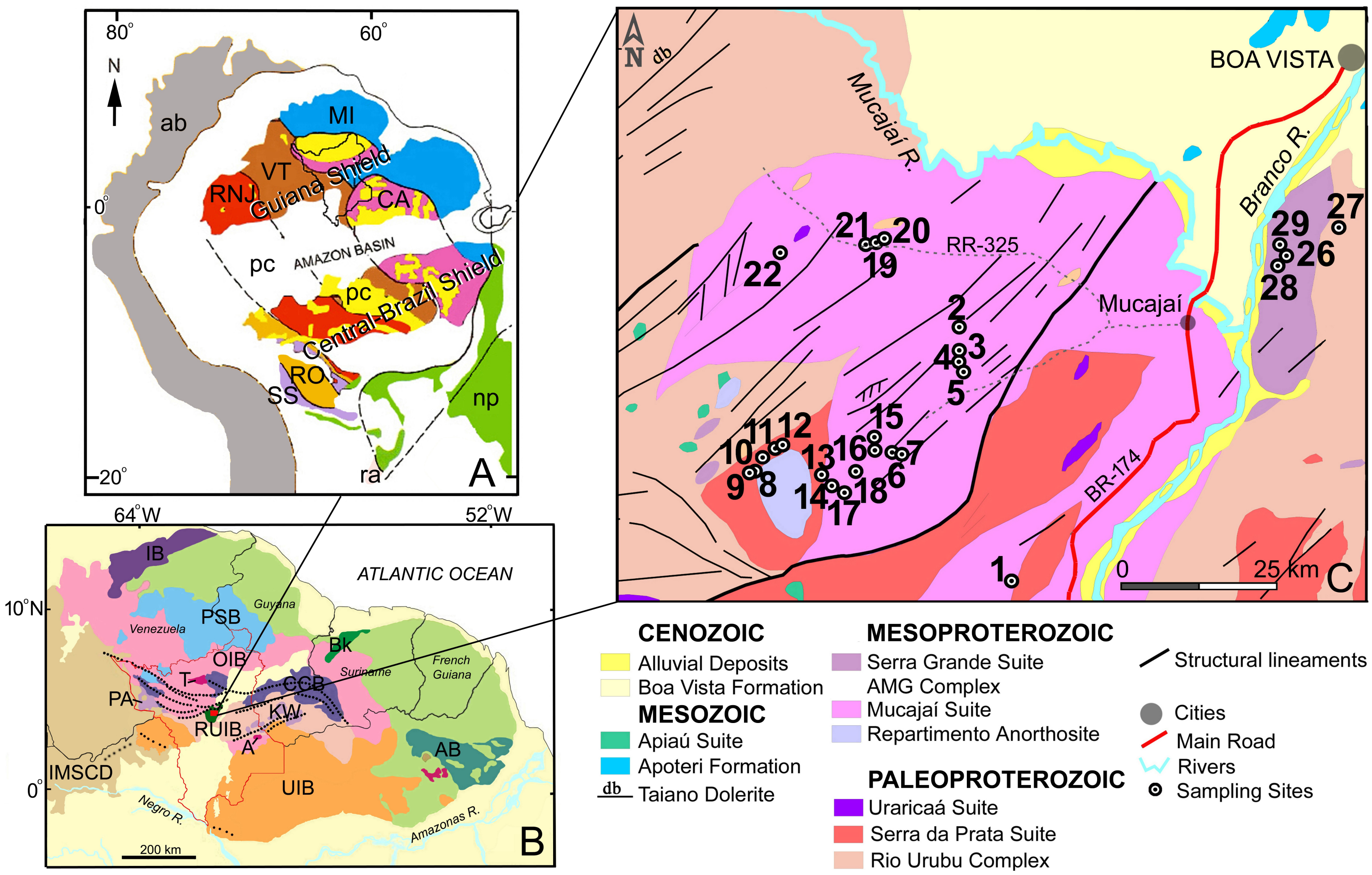

80°
60°
N
ab
MI
VT
RNJ
Guiana Shield
CA
0°
pc
AMAZON BASIN
pc
Central-Brazil Shield
RO
SS
np
-20°
ra
A
64°W
52°W
IB
ATLANTIC OCEAN
10°N
PSB
Guyana
Venezuela
OIB
Bk
Suriname
French Guiana
T
CCB
PA
KW
RUIB
A
AB
IMSCD
UIB
0°
Negro R.
Amazonas R.
200 km
B
N
db
Mucajaí R.
BOA VISTA
Branco R.
21
20
RR-325
19
22
29
27
26
28
2
Mucajaí
4
3
5
15
11
12
10
13
16
7
9
8
6
14
18
17
BR-174
1
0
25 km
C
CENOZOIC
Alluvial Deposits
Boa Vista Formation
MESOZOIC
Apiaú Suite
Apoteri Formation
db
Taiano Dolerite
MESOPROTEROZOIC
Serra Grande Suite
AMG Complex
Mucajaí Suite
Repartimento Anorthosite
PALEOPROTEROZOIC
Uraricaá Suite
Serra da Prata Suite
Rio Urubu Complex
Structural lineaments
Cities
Main Road
Rivers
Sampling Sites

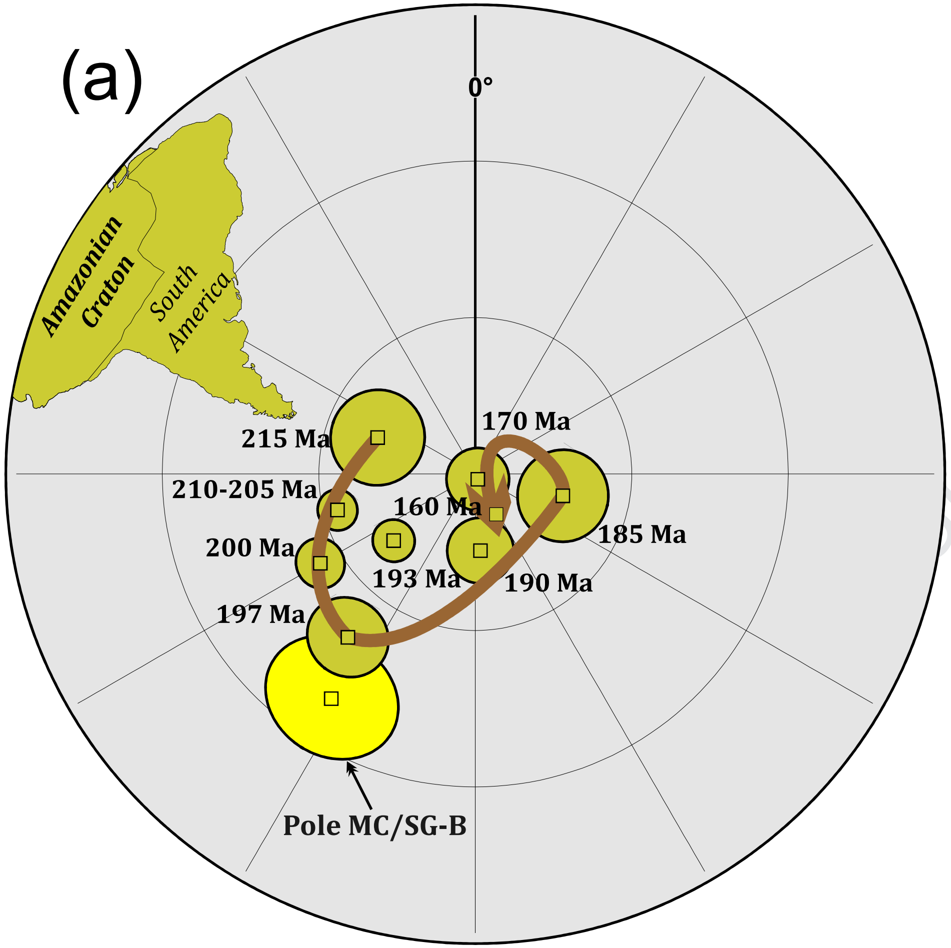
(a)
0°
Amazonian Craton
South America
215 Ma
210-205 Ma
200 Ma
197 Ma
160 Ma
193 Ma
170 Ma
185 Ma
190 Ma
Pole MC/SG-B

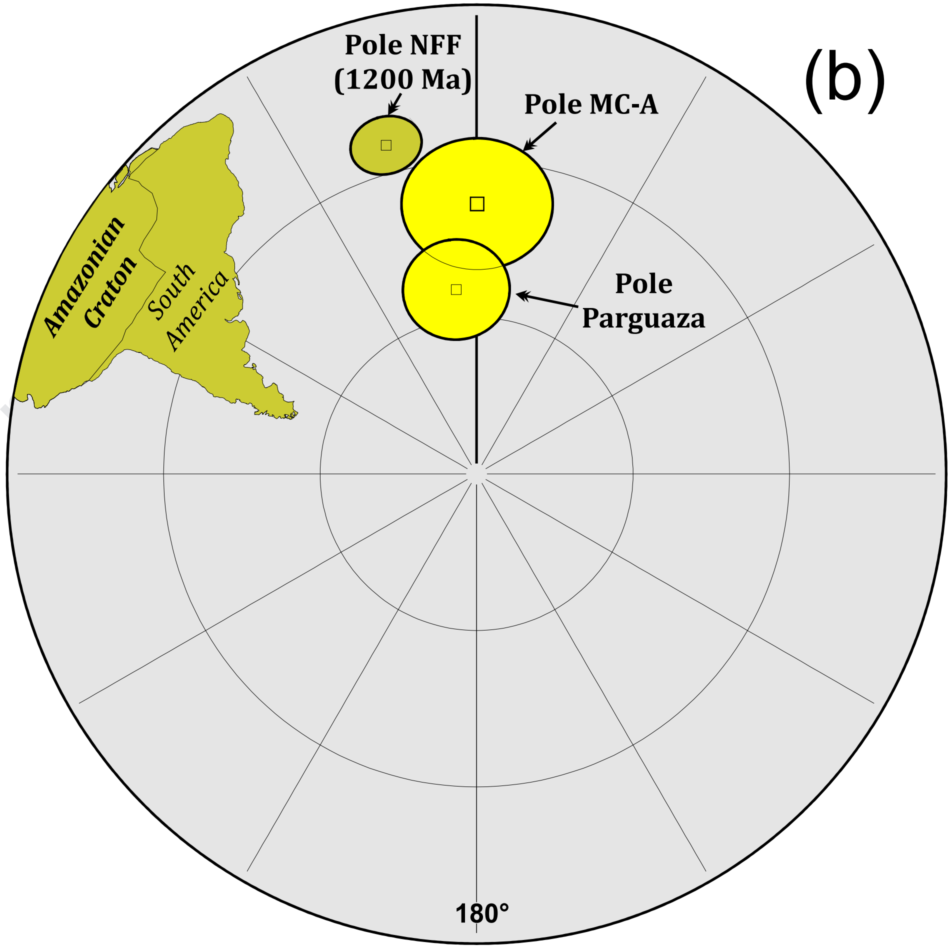
(b)
Pole NFF (1200 Ma)
Pole MC-A
Pole Parguaza
Amazonian Craton
South America
180°

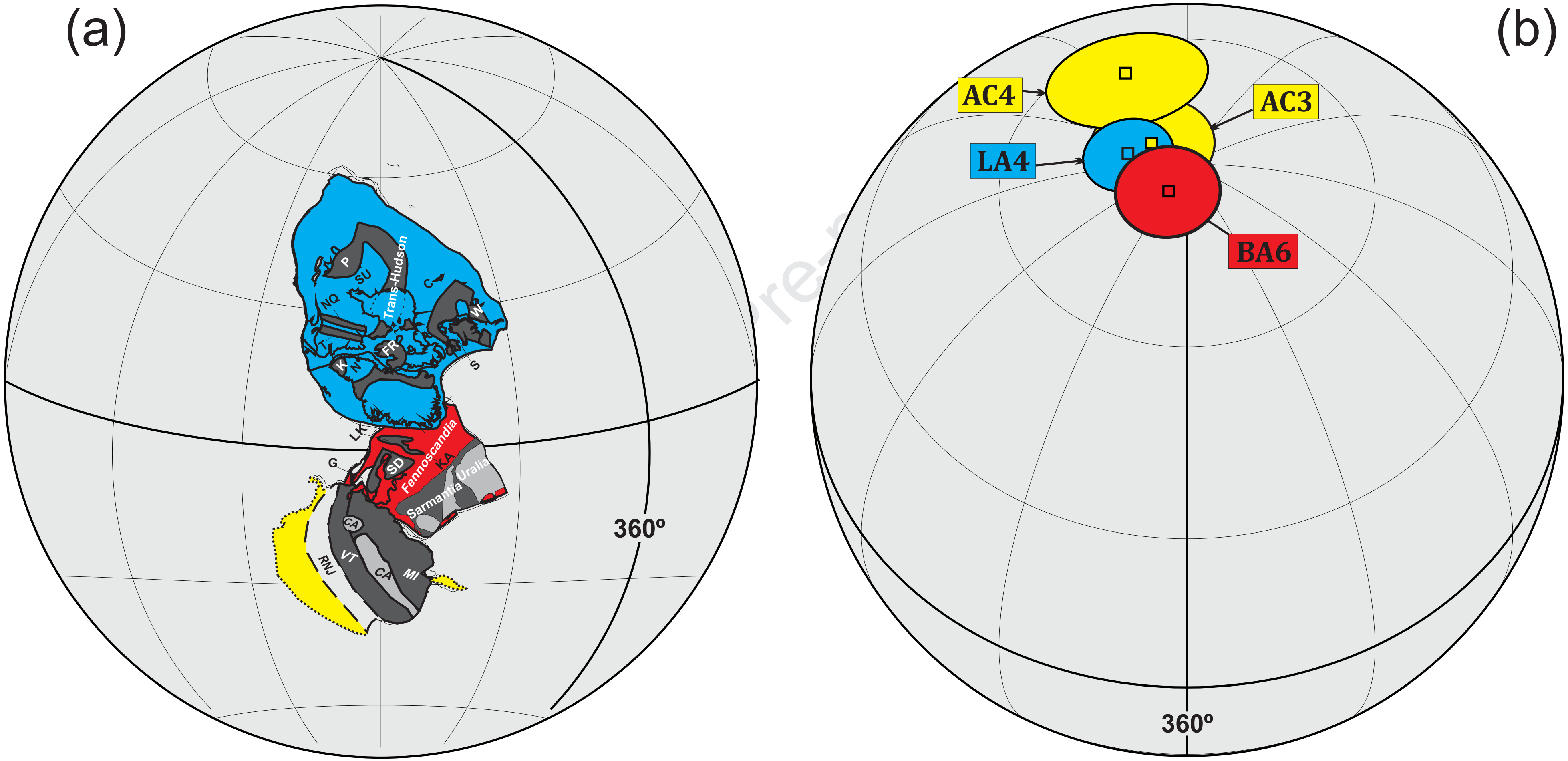
(a)
P
SU
Trans-Hudson
NQ
C
W
FR
K
S
LK
G
SD
Fennoscandia
KA
Uralia
Sarmantia
CA
VT
RNJ
CA
MI
360º
(b)
AC4
AC3
LA4
BA6
360º

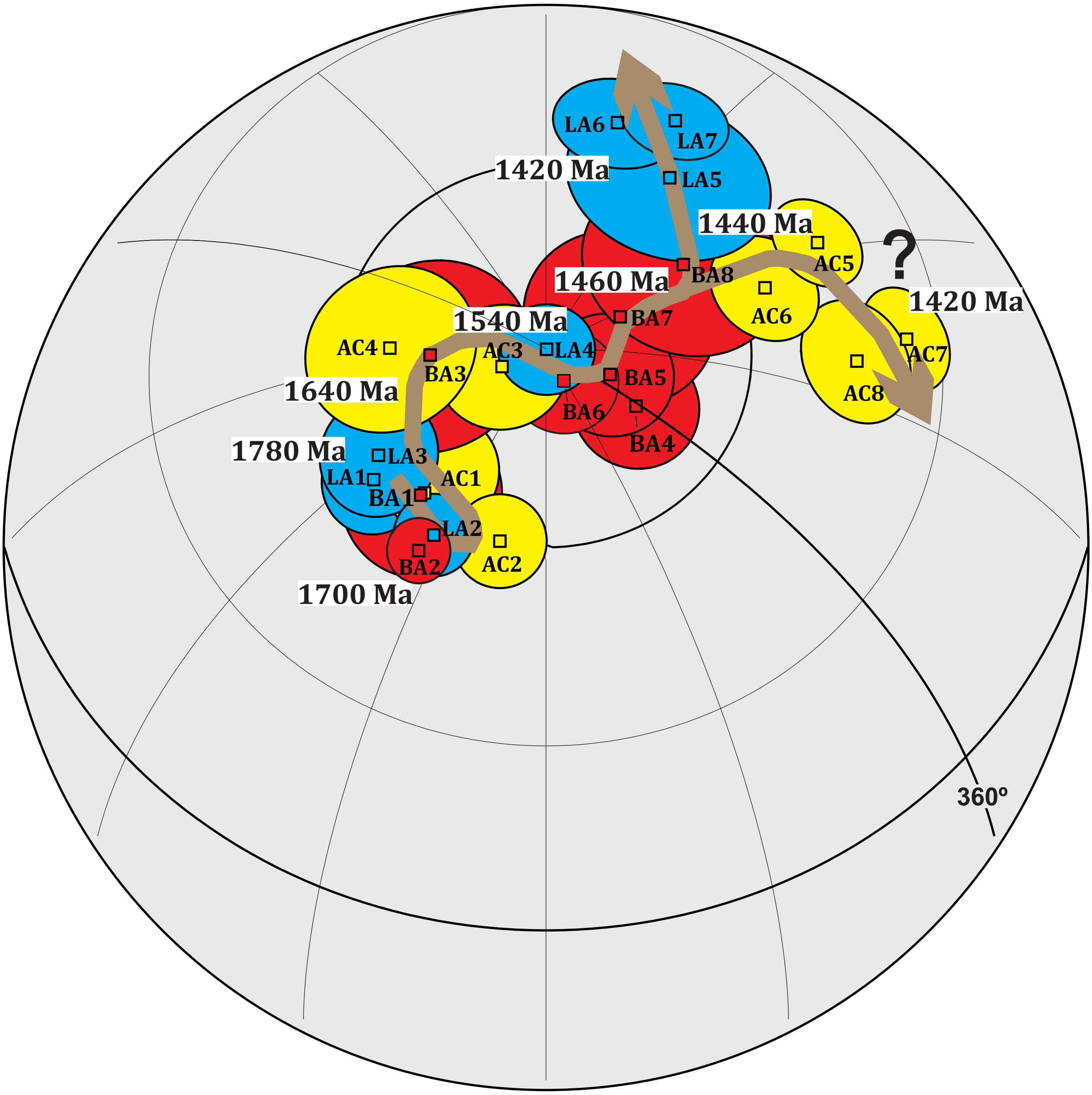

LA6
LA7
1420 Ma
LA5
1440 Ma
AC5
?
1460 Ma
BA8
1420 Ma
1540 Ma
BA7
AC6
AC4
BA3
AC3
LA4
AC7
BA5
AC8
1640 Ma
BA6
BA4
1780 Ma
LA3
LA1
AC1
BA1
LA2
AC2
BA2
1700 Ma
360º

Journal Pre-proof

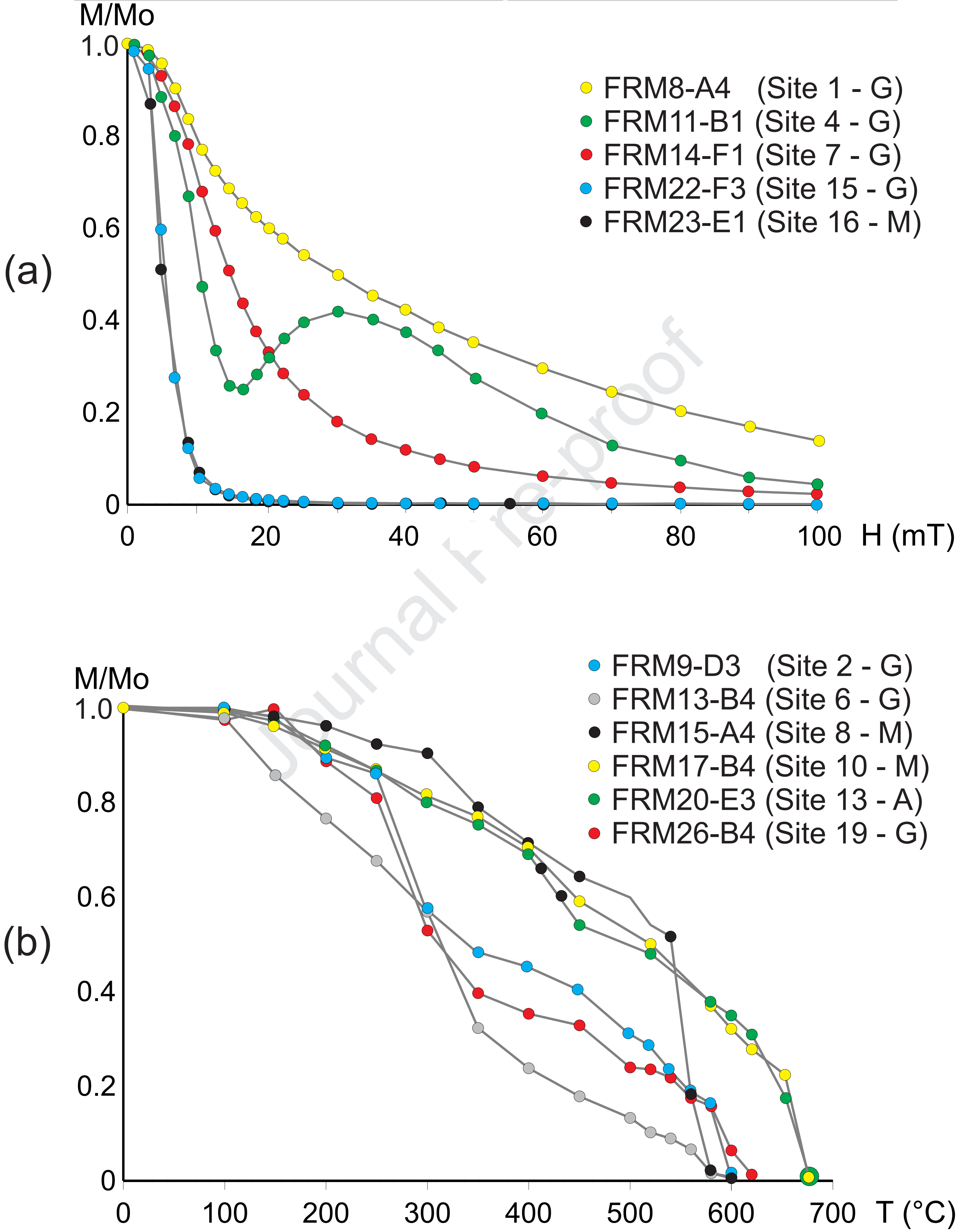

Journal Pre-proof

Journal Pre-proof

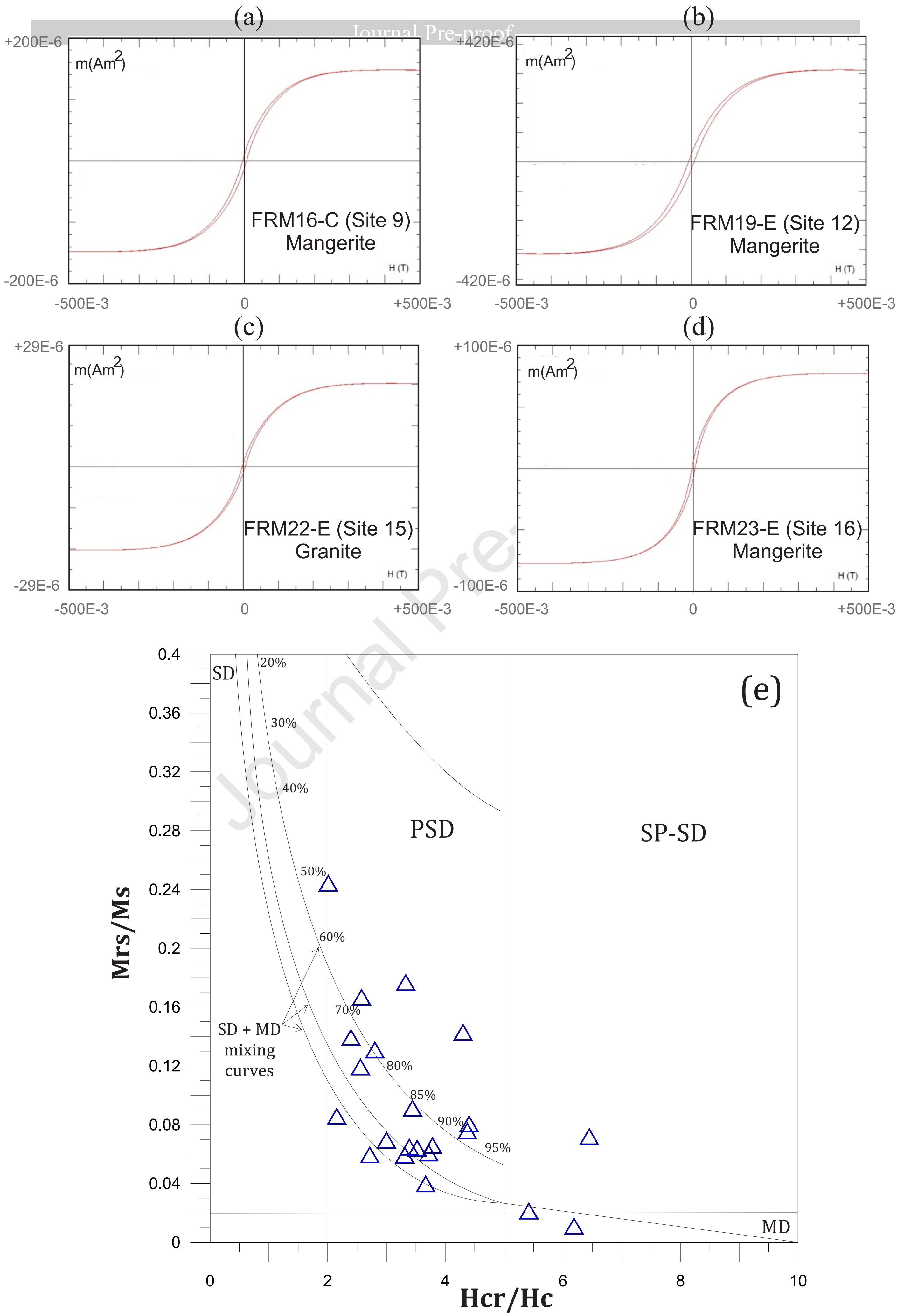

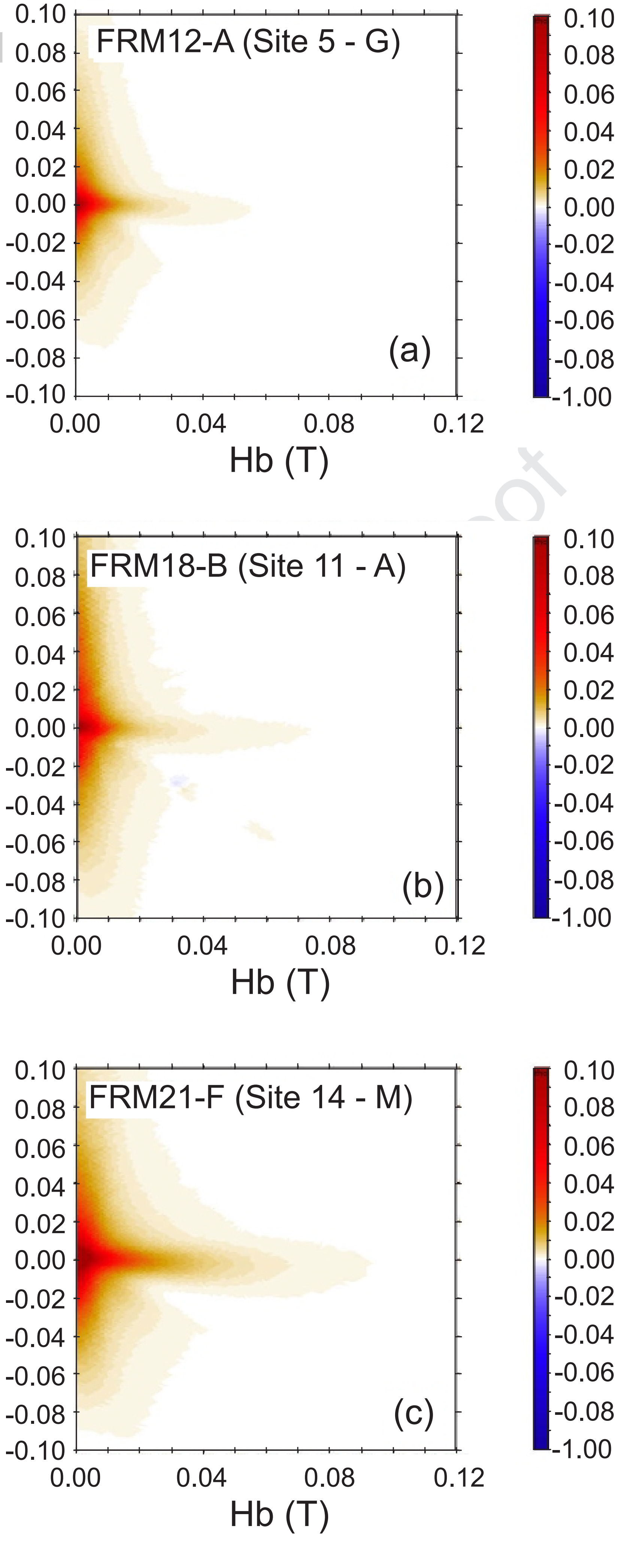
FRM12-A (Site 5 - G)
(a)
FRM18-B (Site 11 - A)
(b)
FRM21-F (Site 14 - M)
(c)
Hb (T)
0.00
0.04
0.08
0.12
0.10
0.08
0.06
0.04
0.02
0.00
-0.02
-0.04
-0.06
-0.08
-0.10
-1.00

Journal Pre-proof

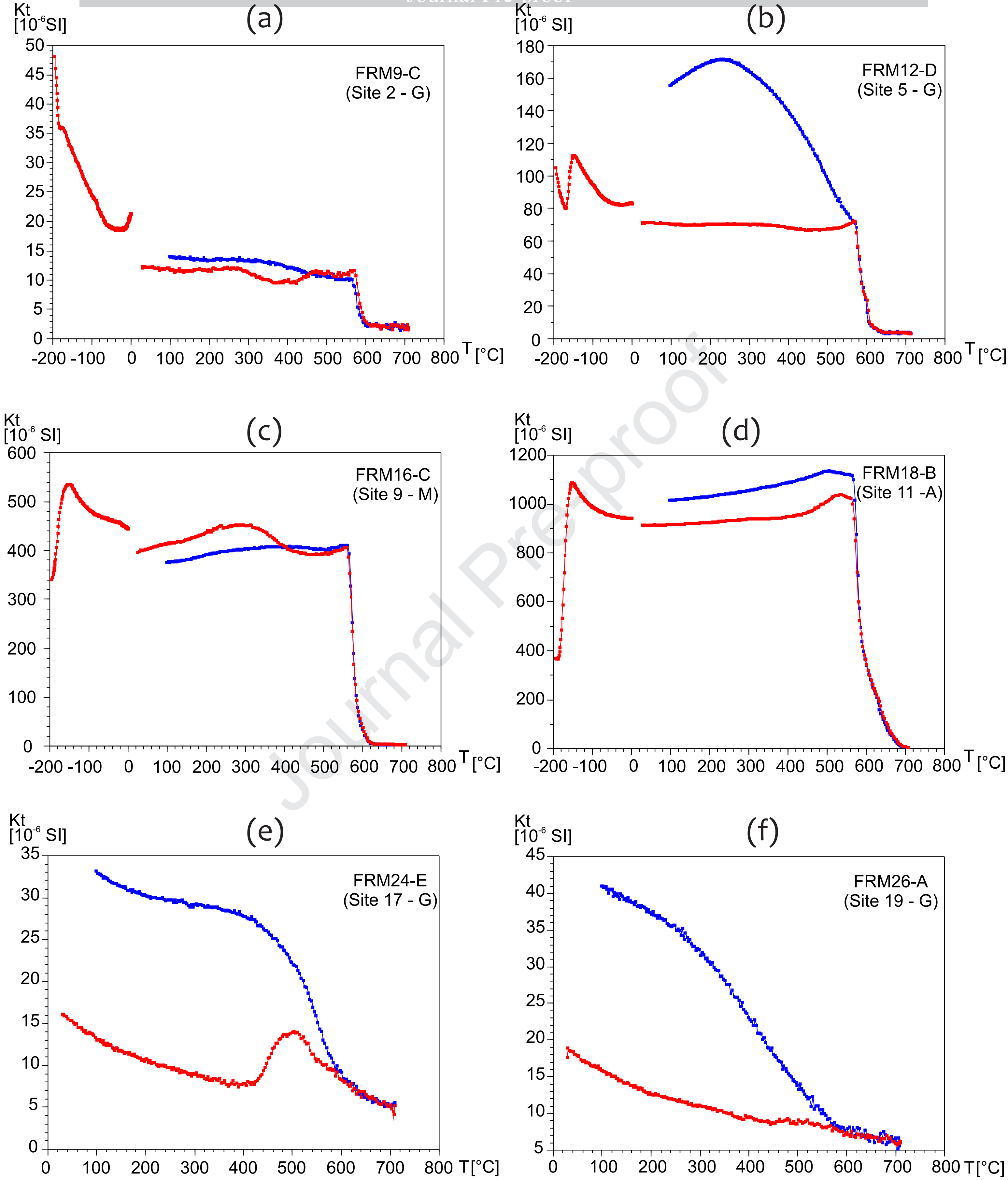

Journal Pre-proof

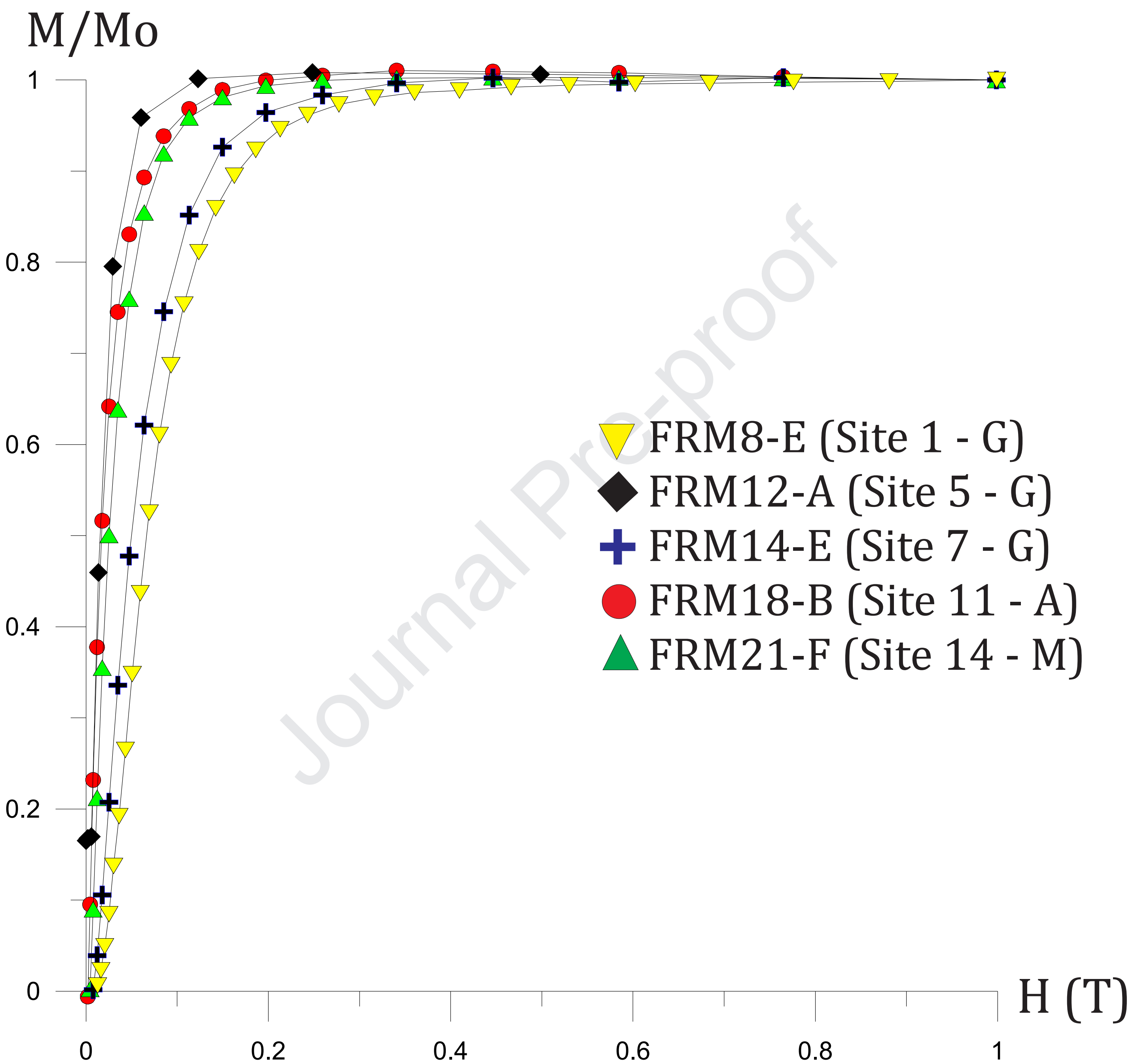

Journal Pre-proof

Journal Pre-proof

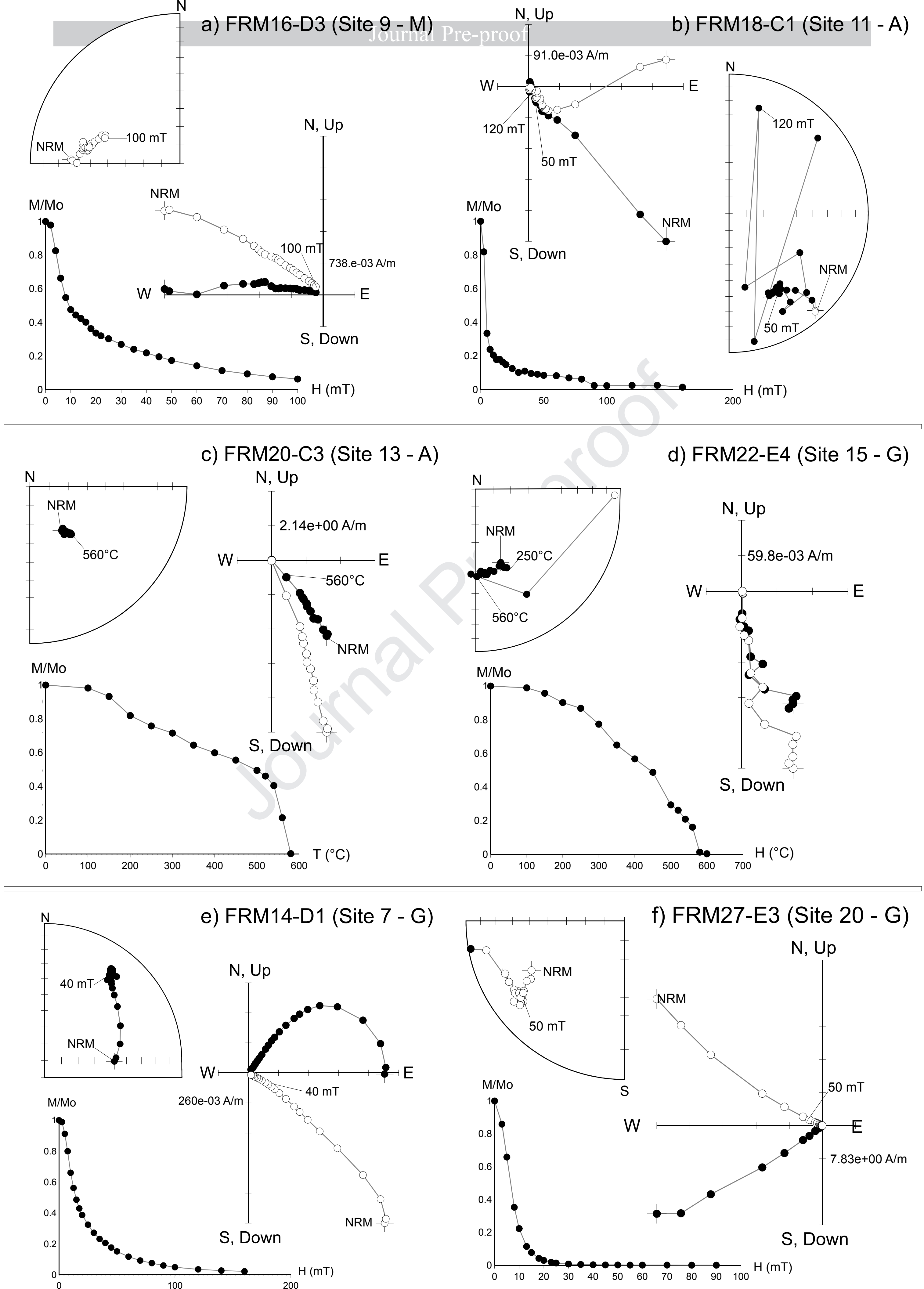

Journal Pre-proof

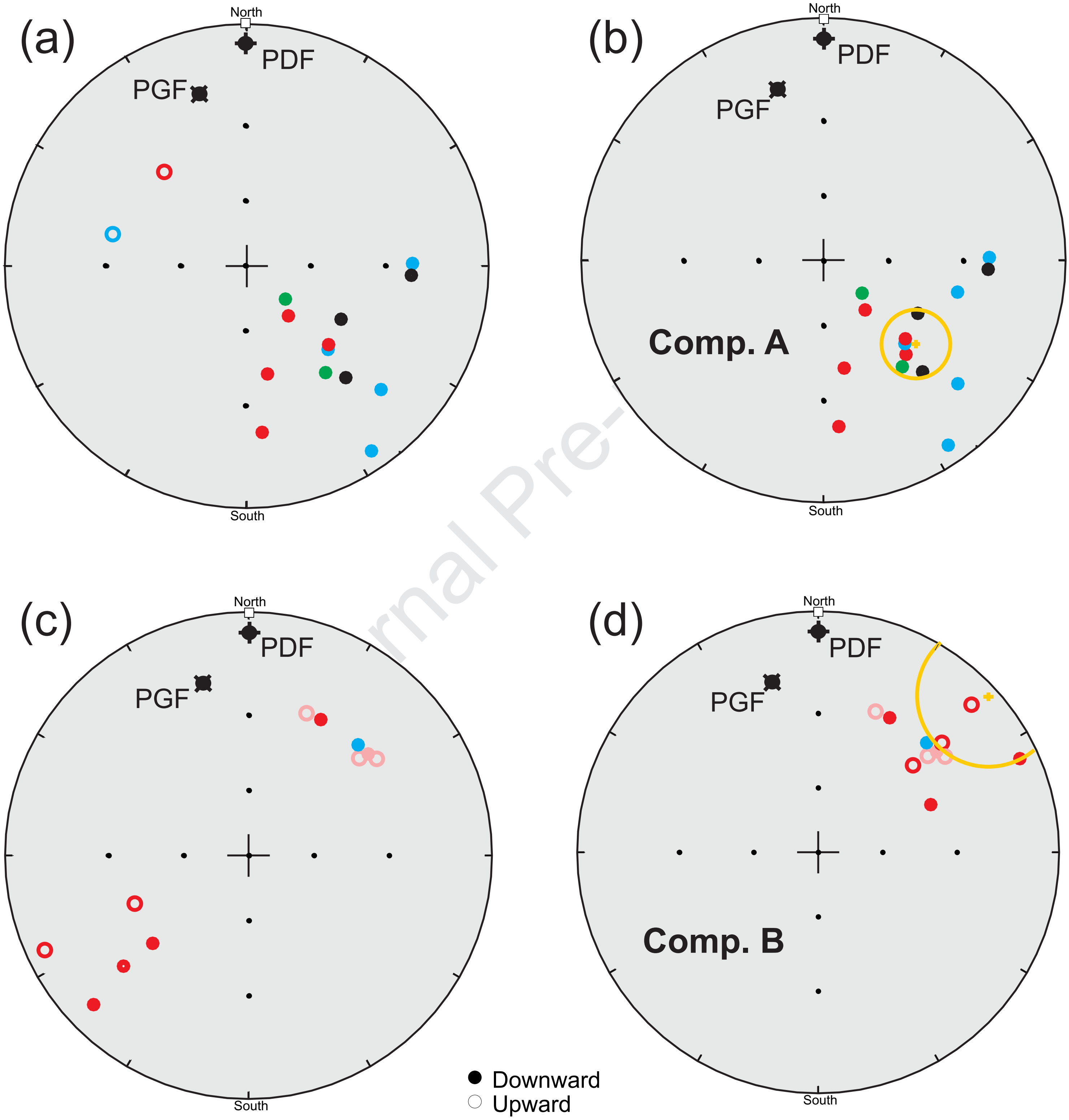
(a)
North
PDF
PGF
South
(b)
North
PDF
PGF
Comp. A
South
(c)
North
PDF
PGF
South
(d)
North
PDF
PGF
Comp. B
South
Downward
Upward

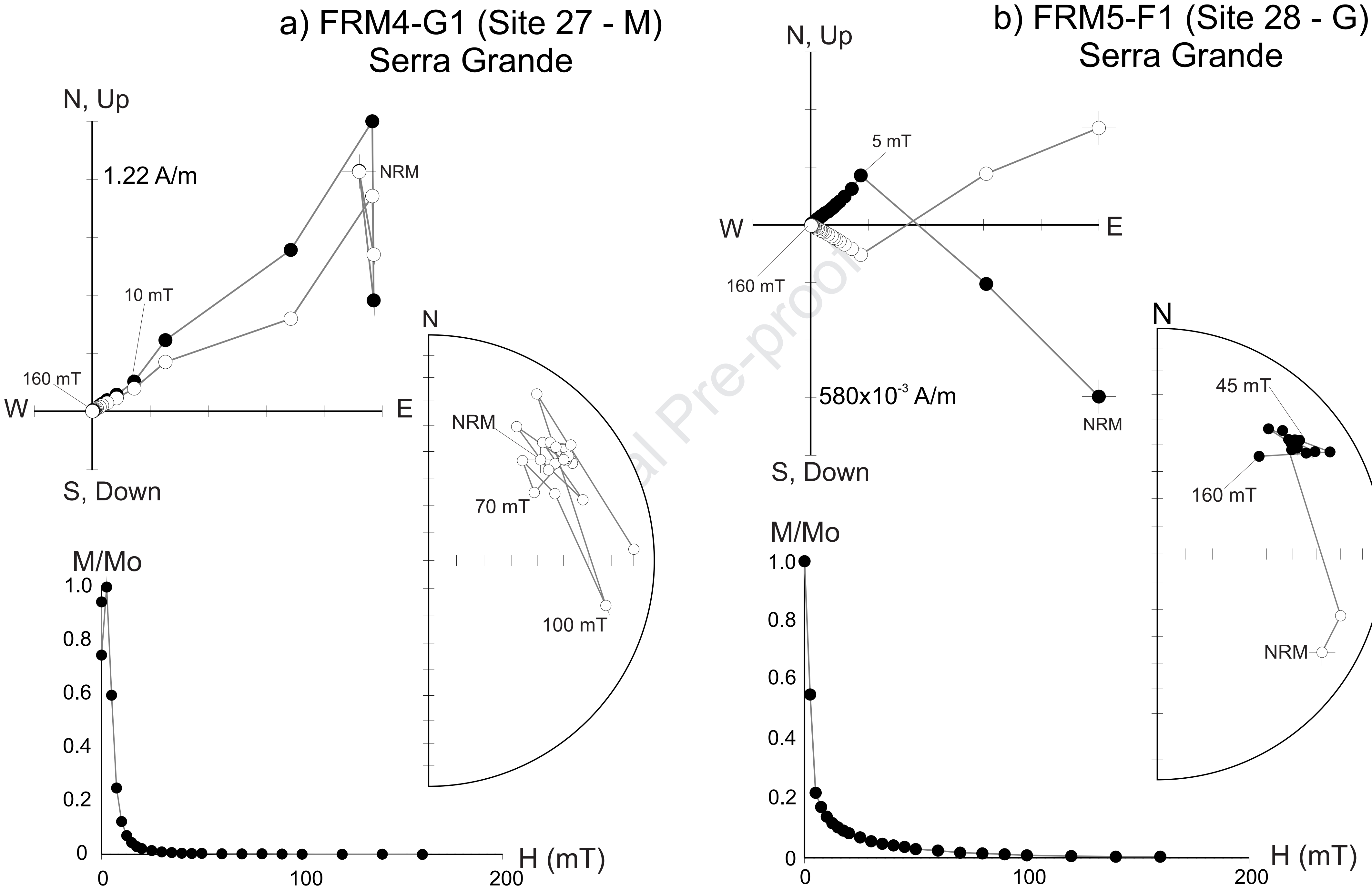

a) FRM4-G1 (Site 27 - M)
Serra Grande
N, Up
1.22 A/m
NRM
10 mT
160 mT
W
E
S, Down
N
NRM
70 mT
100 mT
M/Mo
1.0
0.8
0.6
0.4
0.2
0
0
100
200
H (mT)
b) FRM5-F1 (Site 28 - G)
Serra Grande
N, Up
5 mT
W
E
160 mT
580x10^{-3} A/m
NRM
S, Down
N
45 mT
160 mT
NRM
M/Mo
1.0
0.8
0.6
0.4
0.2
0
0
100
200
H (mT)

Journal Pre-proof

Highlights

Paleomagnetic study of AMG Mucajaí Complex rocks (1535 Ma) from Amazonian Craton.

The Mucajaí pole favours the SAMBA link in a Columbia Supercontinent.

Mucajaí data predict a long-lived SAMBA link forming part of the core of Columbia.

Journal Pre-proof